Developmental Biology 328 (2009) 456–471

Contents lists available at ScienceDirect

Developmental Biology

journal homepage: www.elsevier.com/developmentalbiology

Regulation of mouse embryonic stem cell neural differentiation by retinoic acid

Mijeong Kim [a,c], Ayman Habiba [a], Jason M. Doherty [b], Jason C. Mills [b], Robert W. Mercer [a], James E. Huettner [a,*]

[a] Department of Cell Biology and Physiology, Washington University Medical School, 660 South Euclid Avenue, St. Louis, MO 63110, USA
[b] Department of Pathology and Immunology, Washington University Medical School, 660 South Euclid Avenue, St. Louis, MO 63110, USA
[c] Program in Developmental Biology, Washington University Medical School, 660 South Euclid Avenue, St. Louis, MO 63110, USA

ARTICLE INFO

Article history:
Received for publication 9 December 2008
Revised 20 January 2009
Accepted 3 February 2009
Available online 13 February 2009

Keywords:
Telencephalon
Spinal cord
Serum-free
Transcriptional profile

ABSTRACT

Pluripotent mouse embryonic stem cells (ESCs) derived from the early blastocyst can differentiate *in vitro* into a variety of somatic cell types including lineages from all three embryonic germ layers. Protocols for ES cell neural differentiation typically involve induction by retinoic acid (RA), or by exposure to growth factors or medium conditioned by other cell types. A serum-free differentiation (SFD) medium completely lacking exogenous retinoids was devised that allows for efficient conversion of aggregated mouse ESCs into neural precursors and immature neurons. Neural cells produced in this medium express neuronal ion channels, establish polarity, and form functional excitatory and inhibitory synapses. Brief exposure to RA during the period of cell aggregation speeds neuronal maturation and suppresses cell proliferation. Differentiation without RA yields neurons and neural progenitors with apparent telencephalic identity, whereas cells differentiated with exposure to RA express markers of hindbrain and spinal cord. Transcriptional profiling indicates a substantial representation of transit amplifying neuroblasts in SFD cultures not exposed to RA.

Introduction

In vitro differentiation of embryonic stem cells (ESCs) has attracted wide interest as an experimental system for investigating developmental pathways and mechanisms. In addition, the isolation of human ESCs (Thomson et al., 1998) and human induced pluripotent stem cells (Takahashi et al., 2007; Park et al., 2008) has raised the possibility that *in vitro* differentiation may provide a novel source of cells for tissue replacement or repair (Murry and Keller, 2008). Therapeutic use of ESCs will require robust and reliable methods for producing specific neural cell types. Early work on mouse ESC *in vitro* differentiation was performed in serum-supplemented medium (Doetschman et al., 1985). These experiments found that aggregation of cells into embryoid bodies, combined with exposure to retinoic acid (RA), enhanced the efficiency of ESC conversion to a neural phenotype (Bain et al., 1995; Fraichard et al., 1995; Strübing et al., 1995). Aggregation alone in the presence of serum favours differentiation into non-neural cell types including cardiac cells (Bain et al., 1996), whereas addition of 0.5 to 1 μM RA suppresses non-neural differentiation and instead results in a high proportion of cells becoming neurons or astrocytes (Bain et al., 1995). Neurons produced in this way acquire axonal and dendritic polarity, form functional synapses, and include a mixture of excitatory cells that release glutamate as their transmitter and inhibitory cells that use either GABA or glycine (Strübing et al., 1995; Finley et al., 1996).

Because serum contains a large number of factors that might influence the differentiation process, a number of groups have investigated the *in vitro* conversion of ESCs into neurons, or neural precursors, under serum-free growth conditions (Okabe et al., 1996; Wiles and Johansson, 1999; Finley et al., 1999; Tropepe et al., 2001; Ying et al., 2003; Watanabe et al., 2005; Bouhon et al., 2005). In addition, modifications to the original differentiation procedures have been devised with the goal of enhancing production of specific neural phenotypes including dopaminergic neurons (Kawasaki et al., 2000; Lee et al., 2000), motorneurons (Wichterle et al., 2002), cerebellar neurons (Salero and Hatten, 2007) and oligodendrocytes (Brüstle et al., 1999; Liu et al., 2000). Many of these studies have used media or media supplements with proprietary composition, or they employed serum or cell-conditioned media (Kawasaki et al., 2000; Barberi et al., 2003), which makes it difficult to evaluate the specific requirements for efficient ESC growth and/or differentiation (Cai and Grabel, 2007). Moreover, it is generally recognized that a more comprehensive comparison of the differentiated cell phenotypes produced by these different *in vitro* induction procedures is desirable (Glaser and Brüstle, 2005).

A goal of our work has been to simplify the protocol required for *in vitro* neural induction while preserving cell survival and eliminating exposure to exogenous retinoids. Here we describe a serum-free, retinoid-free, growth medium supporting robust neural differentiation with insulin, transferrin and BSA as the only exogenous protein

* Corresponding author. Fax: +1 314 362 7463.
E-mail address: jhuettner@wustl.edu (J.E. Huettner).

0012-1606/$ – see front matter © 2009 Elsevier Inc. All rights reserved.
doi:10.1016/j.ydbio.2009.02.001

constituents. Neurons derived in this medium exhibit many characteristics of those induced by retinoic acid, but transcriptional profiling revealed substantial differences in gene expression between retinoid-free versus retinoid-exposed cell populations that was confirmed by electrophysiology and immunofluorescence.

Methods

ES cell culture

Murine ESCs were propagated independent of feeder cells in 25 cm^2 tissue culture flasks that had been coated with gelatin (0.1% from bovine skin in sterile water; Sigma). The D3 and CE3 ESC lines were obtained from Dr. David Gottlieb (Adams et al., 2003); the B5 line was obtained from Dr. Andras Nagy (Hadjantonakis et al., 1998). The growth medium for dividing ESCs was Dulbecco's Modified Eagle Medium (DMEM; Life Technologies), which was supplemented with 20% calf serum, nucleosides (30 μM adenosine, cytodine, uridine, guanidine and 10 μM thymidine; Sigma), leukemia inhibitory factor (LIF, 1000 U ml^{-1} ESGRO, murine; Life Technologies) and 2-mercaptoethanol (0.1 mM; Sigma). When cells reached 80 to 90% confluence the medium was removed, the flask was rinsed with divalent-free Earl's balanced salt solution (EBS; Life Technologies), and incubated for 1 min with protease XXIII (1 mg ml^{-1}; Sigma) in divalent-free EBS. Detached cells were triturated gently, collected by centrifugation (70 ×g for 5 min), and then resuspended in 4 ml of complete growth medium. A 1:4 dilution of this cell suspension was used to seed a new flask. All cultures were kept at 37 °C in a 5% CO_2 humidified air incubator.

Neural differentiation

To initiate neural differentiation, ESCs were passaged from the flask with protease XXIII in divalent-free EBS and collected by centrifugation. Cells were resuspended in serum-free differentiation medium (Supplementary Table 1) supplemented with nucleosides (see above) and with 4 mM glutamine, and seeded at a density of 1.5 to 2×10^6 per 5 ml in 5 cm non-adhesive bacteriological Petri plates that had been coated with 0.15% agarose (Sigma, Type II-A). Under these conditions, cells remained suspended and formed aggregates that increased in size to form embryoid bodies. Every 2 d the aggregates were provided with fresh medium as follows. Medium and aggregates were transferred from the Petri dish to a 5 ml round-bottomed tube using a transfer pipette. Fresh medium was added to the empty Petri dish while the aggregates were allowed to settle in the tube for 5–10 min at room temp. Old medium was removed from the tube. The aggregates were resuspended with fresh medium from the Petri dish, transferred back into the Petri dish and returned to the incubator. For some experiments 500 nM all-*trans* RA (Sigma) was added to the medium from d4–8. After 10–12 d, aggregates were dissociated into a single cell suspension and plated onto 35 mm plastic tissue culture dishes or glass cover slips that were coated with a mixture of poly-DL-ornithine (200 μg ml^{-1}; Sigma) and mouse laminin (3 μg ml^{-1}; Gibco). Aggregates were collected in a 5 ml round bottomed tube and incubated for 5 min at room temperature in divalent-free EBS containing protease XXIII (1 mg ml^{-1}). Aggregates were rinsed 2 times with EBS containing 0.1% BSA (Sigma) and 0.1% ovomucoid (Sigma), and then once with SFD medium (Supplementary Table 1). Aggregates were triturated with a fire-polished Pasteur pipette in a total volume of 1–2 ml of SFD medium. Approximately 2–3 fold more cells were obtained from aggregates maintained in SFD medium alone for 12 d than from cultures that were exposed to RA (see Results). For plating, cells were suspended in SFD medium at a density of 3 to 6×10^5 cells ml^{-1} and dispensed onto coated dishes or cover slips. Cells differentiated in SFD medium alone were plated at lower density (~150 cells mm^{-2}) than RA-treated cells (300 cells ml^{-2}) to compensate for differences in proliferation rate (see Results). Cells were allowed to settle and attach for 1 h, then gently rinsed once with SFD medium before adding 0.5 to 1 ml of SFD medium supplemented with 0.25 mM glutamine. Cultures were fed every 2 to 3 d by partial medium replacement. For some experiments, division of non-neuronal cells was inhibited by addition of cytosine arabinoside (10 μM; Sigma) several days after plating. All inductions were performed within 10 passages of thawing from low passage number frozen stocks.

Electrophysiology

Recordings from cells with neuronal morphology were performed as described previously (Bain et al., 1995; Finley et al., 1996). Briefly, cultures were perfused at a rate of 1–2 ml/min with Tyrode's solution: 150 mM NaCl, 4 mM KCl, 2 mM $CaCl_2$, 2 mM $MgCl_2$, 10 mM glucose, and 10 mM HEPES, adjusted to pH 7.4 with NaOH. Pipettes for whole cell recording were pulled from boralex glass capillaries. The internal solution used to record Na and K currents contained 140 mM KCH_3SO_3, or 140 mM K-glucuronate, 10 mM NaCl, 5 mM $MgCl_2$, 200 μM EGTA and 10 mM HEPES, adjusted to pH 7.4 with KOH. For recording agonist-evoked currents, pipettes were filled with 140 mM Cs-glucuronate, 10 mM EGTA, 1 mM ATP (Mg salt), 0.3 mM GTP (tris salt), and 10 mM HEPES, adjusted to pH 7.4 with CsOH. The open tip resistance ranged from 1 to 5 MΩ. Drug solutions were applied to the cells using an array of microcapillary tubes. The time constant for exchange of the external solution was 30–50 ms. Excitatory and inhibitory agonists were dissolved in 160 mM NaCl, 2 mM $CaCl_2$, 0.5 μM tetrodotoxin (TTX, Sigma) and 10 mM HEPES, adjusted to pH 7.4 with NaOH.

Current was recorded with an Axopatch 200A amplifier (Axon Instruments), filtered at 1 to 5 kHz (−3 db, 4 pole Bessel), and digitized at 10 to 20 kHz. Current traces were corrected for leak and capacity using scaled current evoked by an 8 to 10 mV hyperpolarizing step from the holding potential. Membrane potentials were corrected for the junction potential between the internal solution and the Tyrode's solution in which seals were formed. This potential was −10 mV for pipettes containing Cs-glucuronate. All experiments were performed at room temperature.

Immunofluorescence

ESC aggregates or monolayer cultures of differentiated cells were rinsed with Tyrode's solution and incubated for 15–20 min at room temperature in 0.1 M Na Phosphate, pH 7.4, containing 4% paraformaldehyde and for some experiments 0.1% glutaraldehyde. After three rinses with Tris-buffered saline, pH 7.4, aggregates were equilibrated with 30% sucrose, collected in an inverted pyramidal mold (Polysciences) and frozen on dry ice. Aggregates frozen in sucrose were bonded to the chuck with O.C.T. compound (Tissue-Tek), cryosectioned (6 μm) and mounted on Snowcoat X-tra slides (Surgipath). Mounted sections and fixed, rinsed monolayer cultures were incubated for 30 min at room temperature with blocking solution (BS): PBS containing 1% normal goat serum, 0.02% sodium azide, and 0.1% Triton X-100; and then incubated overnight at 4 °C (or in some cases for 2 h at room temperature) with primary antibodies diluted in BS. Samples were rinsed three times with PBS and incubated for 1 h at room temperature with fluorescent conjugated secondary antibodies diluted in BS. They were then rinsed three times with PBS and examined under epi-illumination with appropriate filters. Primary and secondary antibodies and dilutions are reported in Supplementary Table 2. Images were acquired with a Nikon Eclipse E600 microscope with 10×, 40× and 60× objectives (0.3, 0.8 and 1.0 N. A., respectively). Image analysis and quantification was performed with MetaMorph software (Universal Imaging). Most figure panels show sections that did not exceed the field of view of the camera (Photometrics CoolSNAP ES).

RT-PCR

Total RNA was isolated from differentiated ESC cultures using the RNeasy kit (Qiagen) and quantified by optical density. Reverse transcription and PCR were performed according to the manufacturer's protocol using the OneStep RT-PCR Kit (Qiagen) and 50 ng of RNA. In brief, reverse transcription for 30 min at 50 °C was immediately followed by PCR activation at 95 °C for 15 min, then 30 cycles of denaturation at 94 °C for 1 min, annealing at 50 °C for 1 min and extension at 72 °C for 1 min. Final extension was at 72 °C for 10 min. The following primers were used:

glycine receptor (GlyR)
GlyR α1 forward: 5′-TGTACATCCCCAGCCTGCTCATCGTCATC-3′
reverse: 5′-GAGGCGGGTTAGTGGTGTTGTTGTTGTTGG-3′
GlyR α2 forward: 5′-CACCTTGCCCCAGTTTATTTTGAA-3′
reverse: 5′-GATGCCCTGGAACCTGAACTCTGTGTAG-3′
GlyR α3 forward: 5′-CTTTCGGACACTAGTTTCTGGATTTTAC-3′
reverse: 5′-AGTTAGCCCCCTTCTCATTAGCA-3′
GlyR α4 forward: 5′-AGGGGCCAACTTCCATGAGGTGAC-3′
reverse: 5′-CAAGGCAGCAAATACAAAGAGCAGGCATACAGC-3′
GlyR β forward: 5′-CTCATTGCCTGCCTGCTCTTCGGGTTTG-3′
reverse: 5′-GATGCGCTTGGCTGCTGTTGGGATGA-3′
GAPDH forward: 5′-GAGGCCGGTGCTGAGTATGTC-3′
reverse: 5′-TCCACCACCCTGTTGCTGTAG-3′.

Microarray analysis

Total RNA was isolated using Trizol reagent (Life Technologies) from replicate cultures of undifferentiated ESCs and from cells aggregated in suspension 12 d in SFD medium, with or without exposure to RA (d4–d8), then dissociated and maintained 6 d in plated cultures. RNA from each sample was used to generate biotinylated-fragmented cRNA probes using a Bioarray High Yield RNA transcript labelling kit (Enzo Biochem, New York). Hybridized Affymetrix gene chips (MOE430v2), which represent approximately 39,000 transcripts, were washed and stained according to the manufacturer's protocols, then scanned in the Affymetrix GeneChip array scanner by the Siteman Cancer Center Multiplexed Gene Analysis Core at Washington University Medical School. Array images were analyzed using Affymetrix Microarray Suite version 5.0. Gene expression values were normalized to the median intensity array before model-based analysis using dChip software (Li and Wong, 2001). Using undifferentiated ESCs as a baseline, genes were identified as enriched in differentiated cells if they satisfied both of the following criteria: 1) a ~2-fold increase in mean normalized intensity level (1.2 fold 90% lower confidence bound, see Li and Wong (2001), Ramalho-Santos et al. (2002)) and 2) an absolute difference in mean normalized intensity level >100. This second criterion sets a baseline for expression in the differentiated population to screens out genes with very low expression in both undifferentiated and differentiated populations. Genes identified as common among all three populations had mean normalized intensity values >100 and were identified as "present" by MAS 5.0 in at least one of the replicate samples from each population. Gene Function Enrichment analysis was performed in dChip. Hierarchical clustering based on population Gene Ontology term representation was performed with GOurmet software (Doherty et al., 2006, 2008).

BrdU labelling

For cell proliferation analysis, bromodeoxyuridine (BrdU, Sigma) was added to aggregates at 10 μg ml^{-1} every 4 h for 24 h. Aggregates were harvested at 0 h, 1 h, 2 h, 4 h, 6 h, 8 h and 24 h after BrdU treatment, and fixed for 20–30 min at room temperature with 4% paraformaldehyde in 0.12 M sodium phosphate, pH 7.0. Aggregates were cryosectioned, post-fixed in 4% paraformaldehyde in 0.12 M sodium phosphate, pH 7.0, and treated with 2N HCl for 10 min at 37 °C. For cultured cells, BrdU was applied for 2 h prior to fixation with 4% paraformaldehyde in 0.1 M sodium phosphate, pH 7.0, for 10–15 min. Immediately before staining, cultured cells were post-fixed for 15 min at room temperature with 4% paraformaldehyde in 0.12 M sodium phosphate, pH 7.0, then treated with 2N HCl for 30 min at 37 °C. Cultures and slide-mounted sections were neutralized by room temperature incubation for 20 min in borax solution: 55% 0.2 M boric acid + 45% 0.05 M borax. After 3 washes with PBS, samples were blocked with PBS containing 1% goat serum and 0.1% Triton X-100 for 30 min, then incubated for 1–2 h at room temperature with mouse anti-BrdU (1:400, Boehringer Mannheim). Goat anti-mouse Cy3-conjugated secondary antibodies were used to detect BrdU-positive cells. Cell nuclei were counterstained with Hoechst33342 (2.5 μM). Counts were performed to quantify the number of cells that incorporated BrdU as a percentage of Hoechst 33342 stained nuclei (23–25 aggregate sections or 34 plated culture fields for each time point).

Statistical analysis

Unless otherwise specified, data are expressed as mean ± sem. Statistical analysis was performed with SigmaStat (Systat Software) or with the appropriate functions in Excel (Microsoft). Significance was assigned for p values < 0.05.

Results

Neural differentiation

In a previous work (Finley et al., 1999) we demonstrated relatively efficient neural differentiation when ESC aggregates were maintained for 8 d in serum-free Neurobasal Medium plus the B27 supplement, which contains 20 different ingredients including retinyl acetate (Brewer et al., 1993); however, generation of neurons was dramatically curtailed when complete B27 supplement was replaced with B27 that lacked retinyl acetate (Finley et al., 1999). To investigate the effects of retinoids on ESC neural differentiation, we developed a modification of earlier serum-free induction media (Wiles and Johansson, 1999; Tropepe et al., 2001; Ying et al., 2003) that lacks exogenous retinoids and avoids the use of proprietary growth supplements or media formulations (Supplementary Table 1).

To initiate induction, feeder-free ESC monolayers were detached with protease, rinsed extensively with balanced salt solution, suspended in serum-free differentiation medium (SFD; Supplementary Table 1), and dispersed into non-adherent Petri dishes. Under these conditions the cells formed floating aggregates that gradually enlarged by cell division. Expression of Oct3/4, which defines the undifferentiated state (Niwa et al., 2000), progressively declined (Supplementary Fig. 1), while there was a gradual increase in cells expressing proteins associated with neurons or neural precursors including nestin (Lendahl et al., 1990) and β-3-tubulin (Caccamo et al., 1989) (Supplementary Fig. 1). Cells maintained exclusively in SFD medium acquired neural properties over a time course of 10–12 d, whereas addition of 0.5 μM RA from d4–d8 speeded differentiation, as evidenced by a higher proportion of β-tubulin-expressing cells at earlier time points. Aggregates maintained in suspension for 12 d were dissociated to single cells and plated onto laminin plus poly-DL-ornithine coated tissue culture plastic in SFD medium with reduced glutamine to avoid conversion to excitotoxic glutamate (Newcomb et al., 1997). Immunofluorescent staining 3–6 d after plating revealed a high proportion of β-3-tubulin positive neurons, as well as glial fibrillary acidic protein (GFAP) positive astrocytes, in cultures induced

with SFD medium alone, or with addition of RA during d4–d8 as aggregates (Figs. 1A–E).

Polarity

Mature neurons exhibit distinct axonal and somatodendritic compartments; the degree of polarity increases with neuronal maturation (Caceres et al., 1986; Dotti et al., 1988). We visualized the axonal marker growth associated protein 43 (GAP43) and the somatodendritic marker microtubule-associated protein 2 (MAP2) at several time points after plating. On d1 in culture, both GAP43 and MAP2 were observed within the same neurites of cells induced with or without exposure to RA (Figs. 1F, I, L). Segregation into separate axonal and dendritic compartments was well advanced by d3 after plating in cells induced with RA (Figs. 1J, L). In cells induced without RA, however, colocalization of axonal and dendritic markers declined more gradually, remaining higher than for RA treated cells at d6 after plating (Figs. 1H, L). Full segregation of GAP43 and MAP2 required 7–10 d in cultures differentiated without RA (Supplementary Fig. 2). Thus, cells exposed to RA establish polarity more rapidly than cells induced in SFD medium alone, consistent with the idea that neurons induced with RA are more mature, or mature more rapidly, than those which differentiate without RA.

Transmitter phenotype

To evaluate neurotransmitter phenotypes we used immunofluorescence with antibodies to the inhibitory neurotransmitter γ-aminobutyric acid (GABA) and to the GABA synthetic enzyme, glutamic acid decarboxylase (GAD), as markers for GABAergic neurons (Chang and Gottlieb, 1988). Cells induced without RA generated a higher proportion of cells that were double-labelled for β-3-tubulin and either GABA (37.2 ± 2.6%, $n = 27$) or GAD (42.8 ± 2.7%, $n = 30$) than cells induced with RA (24.4 ± 1.5%, $n = 22$) and (22.6 ± 1.2%, $n = 30$), respectively (Figs. 2A–D, G). Essentially all GAD or GABA positive cells were also positive for β-3-tubulin regardless of RA exposure. Double immunofluorescence with anti-GAD and anti-GABA demonstrated co-staining in the majority of cells, although the anti-

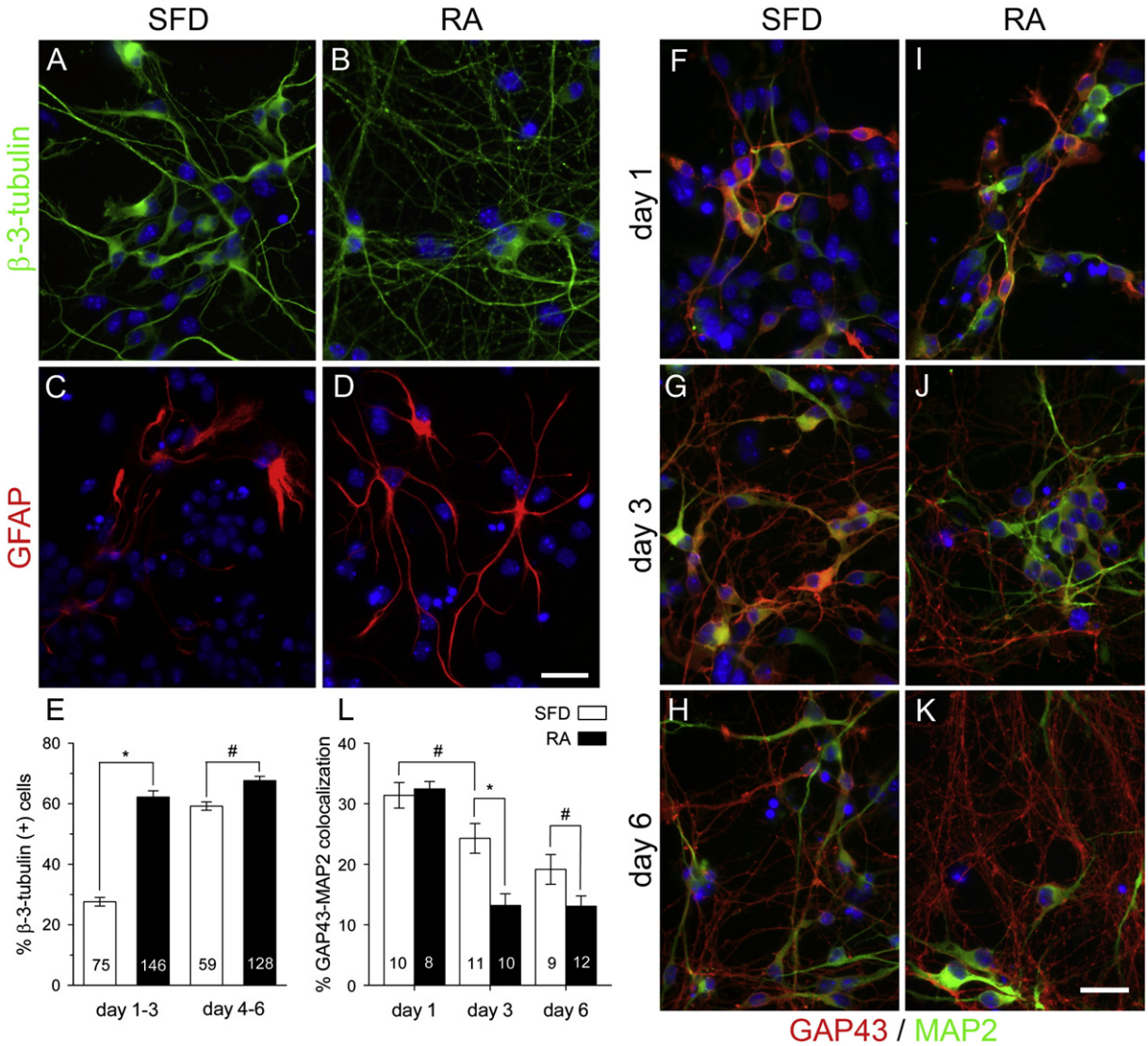

Fig. 1. Neural differentiation with and without retinoic acid. Immunofluorescence for β-3-tubulin (green) (A, B) and GFAP (red) (C, D), together with Hoechst 33342 nuclear counterstaining (blue) in plated cultures differentiated in SFD medium without RA (A, C) or with RA (B, D). Scale bars: 25 μm. (E) Plots of β-3-tubulin immunofluorescent cells as a percent of Hoechst stained cell nuclei (mean ± sem) within the first 3 d or d4–d6 after plating. Double immunofluorescence for GAP43 (red) and MAP2 (green) in cells induced without RA (F, G, H) or with RA (I, J, K), fixed 1 d (F, I), 3 d (G, J), or 6 d (H, K) after plating. Scale bar: 25 μm. (L) Percent GAP43/MAP2 colocalization (mean ± sem). Cultures from RA-treated inductions (solid bars) included a higher proportion of β-3-tubulin-positive neurons and established a polarized distribution of axonal and somatodendritic markers earlier than cells differentiated in SFD medium alone (open bars). *$p < 0.01$; #$p < 0.05$.

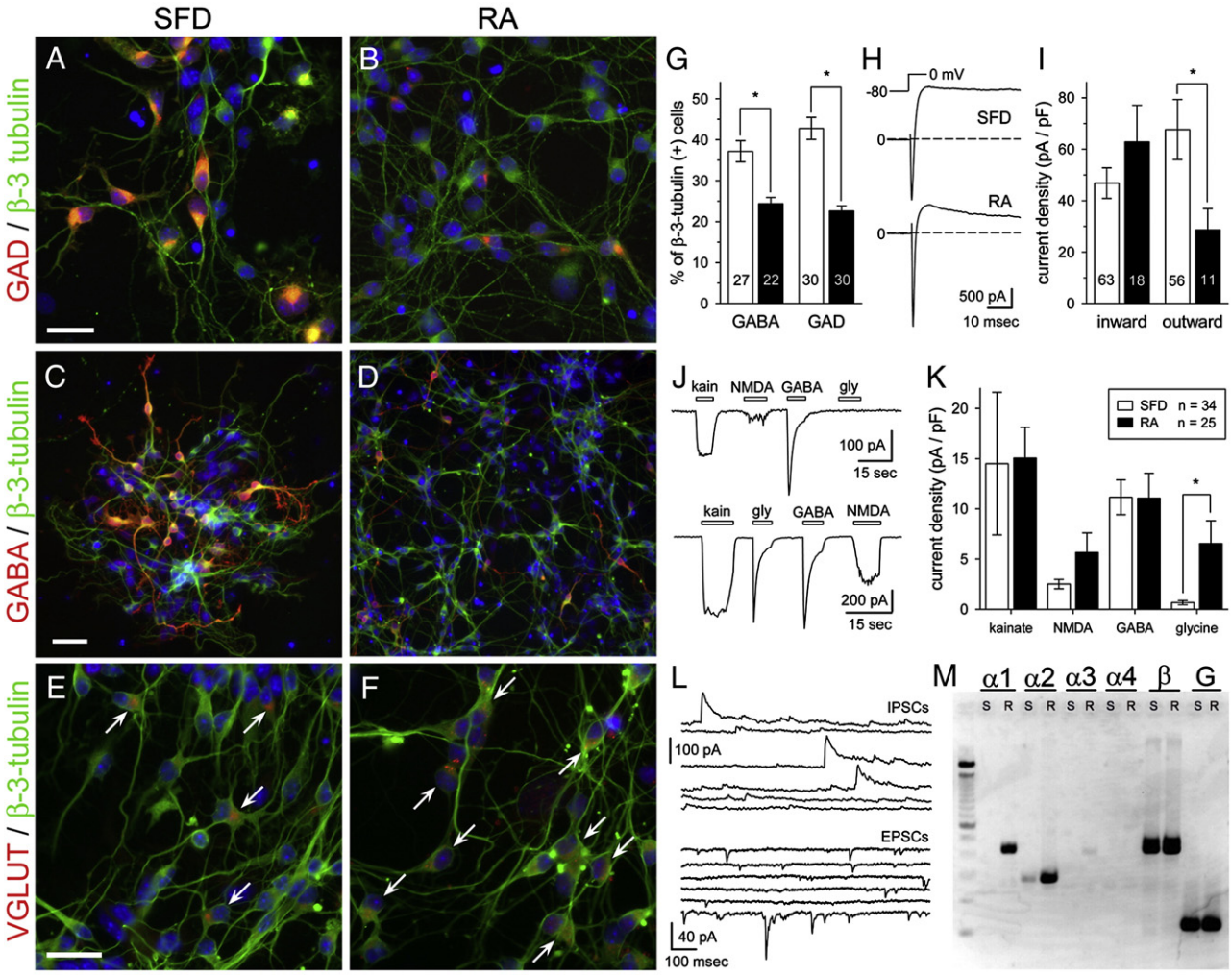

Fig. 2. Transmitter phenotypes and electrophysiological properties. Double immunofluorescence for β-3-tubulin (green) and either glutamic acid decarboxylase (GAD; A, B) or GABA (red) (C, D) in cells induced without RA (A, C), or with RA (B, D). Double immunofluorescence for β-3-tubulin (green) and vesicular glutamate transporter 1 (VGLUT1) (red), a marker for glutamatergic neurons, in cells induced without (E) or with RA (F). A higher proportion of cells induced with RA was glutamatergic (arrows). Scale bar: 25 μm. (G) Percent of β-3-tubulin-positive neurons co-labelled with anti-GABA or anti-GAD in cells induced with SFD medium alone (open bars) or with exposure to RA (solid bars). Cells induced without RA generated a higher proportion of GABAergic neurons than cells induced with RA. $*p<0.01$. (H) Whole-cell currents evoked by a voltage step from −80 to 0 mV. (I) Peak inward sodium and outward potassium current densities in neurons differentiated in SFD medium alone (open bars) or with RA (solid bars). (J) Whole-cell currents evoked by 100 μM kainate, GABA, glycine and by 40 μM NMDA in cells induced without (top) or with (bottom) RA. (K) Plots of agonist-evoked current density. All four agonists evoked current in neurons derived from ESCs exposed to RA; however, neurons generated in SFD medium alone failed to express functional glycine receptors. (L) Spontaneous inhibitory synaptic currents recorded at 0 mV and excitatory synaptic currents recorded at −80 mV in neurons differentiated in SFD medium alone. (M) Reverse transcription-polymerase chain reaction (RT-PCR) analysis of the expression of glycine receptor subunits, α1, α2, α3, α4, and β in cells induced without RA or with RA. S: cells induced in SFD medium alone; R: cells induced in SFD medium with RA from d4–d8 in suspension. Glyceraldehyde-3-phosphate dehydrogenase (lane G) was used as a control. Cells induced with RA expressed all of the glycine receptor subunits except α4, whereas only the β subunit and α2 embryonic subunit were detected in cells induced without RA exposure.

GAD signal was indistinguishable from background in a small percentage of GABA-positive cells (Supplementary Fig. 3). Consistent with the lower proportion of GAD- and GABA-positive neurons, immunofluorescence for the vesicular glutamate transporter 1 (VGLUT1), a marker for excitatory glutamatergic neurons (Bellochio et al., 2000; Takamori et al., 2000), was more prevalent in cultures from RA-treated aggregates (Figs. 2E, F, arrows). Because anti-vGLUT1 only weakly labels the cell soma, however, we did not undertake to quantify the proportions of positive cells.

Electrophysiology

Whole-cell patch clamp recordings were used to compare the physiological characteristics of neurons induced without or with exposure to RA. Nearly all cells with neuronal morphology expressed voltage-gated sodium and potassium currents, when analyzed 7–14 d after plating (Figs. 2H, I). In addition, currents were evoked in the cells by brief applications of GABA, acting on $GABA_A$ receptors, and by kainic acid and NMDA, which are agonists for two different glutamate receptor subtypes (Fig. 2J). Functional synaptic transmission between neurons generated in SFD medium was detected after ~3 weeks in culture (Fig. 2L). Interestingly, the inhibitory neurotransmitter glycine failed to elicit detectible current in the majority of neurons induced in SFD medium without exposure to RA (Figs. 2J, K). By contrast, neurons exposed to RA during induction in SFD medium expressed functional glycine receptors, as previously described for differentiation with serum (Bain et al., 1995).

The difference in glycine-evoked current between cells induced with RA or without RA led us to examine the expression of glycine receptor subunits by RT-PCR. Glycine receptors comprise pentameric subunit complexes that include α and β subunits. Only α subunits generate functional homo-oligomeric glycine receptors; β subunits do not form receptors by themselves (Kuhse et al., 1993). Thus far, four α subunits and one β subunit have been identified. In adult rats the α1 and α3 subunits are highly expressed in the spinal cord and brain stem, and are also found in the superior and inferior colliculi and in

some regions of the thalamus and hypothalamus (Malosio et al., 1991). The α2 subunit is expressed throughout most of the embryonic CNS including cortex, thalamus and hippocampus (Akagi et al., 1991), but declines sharply after birth with more restricted expression in adults, notably in the retina, and in auditory brain stem nuclei (Piechotta et al., 2001). The α4 subunit is a component of embryonic glycine receptors in the spinal cord, sympathetic ganglia and dorsal root ganglia (Harvey et al., 2000). Cells induced with RA expressed all of the subunits except α4, whereas cells induced without RA expressed only small amounts of α2 and the β subunits (Fig. 2M). These results are consistent with our electrophysiological recordings. Together they suggest that cells induced without RA may be physiologically less mature than cells induced with RA, or may correspond to cell types that do not express functional glycine receptors *in vivo*.

Transcriptional profiles

To gain a broader perspective on phenotypic differentiation we used microarray analysis to test for genome-wide transcriptional differences between cells induced with SFD medium alone or with exposure to RA from d4–d8 in suspension (Fig. 3A). For comparison, we also isolated RNA from replicate plates of undifferentiated ESCs. Probes were hybridized to Affymetrix Mouse genome arrays (MOE430v2). Array scans were analyzed with Affymetrix MAS 5.0 software and dChip, a model-based program for pooling and statistical comparison across multiple chip data sets (Li and Wong, 2001).

A common pool of 2496 genes was elevated in cells differentiated with SFD medium alone and in cells that were exposed to RA, including many encoding for known neuronal proteins (Figs. 3B, C; Supplementary Data File #1). In addition, 557 genes were enriched only in cells that underwent differentiation in SFD medium without RA, whereas 1202 genes were enriched only in cultures from inductions that had been exposed to RA. Fig. 3C presents the 50 genes most enriched in the undifferentiated (ES) or the differentiated (SFD, RA) cell populations, sorted from highest to lowest fold enrichment (lower bound). Based on a recent transcriptome analysis of neurons, astrocytes and oligodendrocytes (Cahoy et al., 2008) many of the genes enriched in our differentiated cell populations (SFD, RA) are specific for particular neural cell types. A high proportion of genes enriched in astrocytes is specifically up regulated in cells differentiated with SFD medium alone, whereas many neuron-specific genes are selectively up regulated in cells that received brief exposure to RA (Fig. 3C).

Genes enriched both in ESCs and in cultures differentiated with SFD medium alone (449) included many associated with cell division, such as cyclin A2 and D1, geminin, and wee 1. By contrast, only a few genes were enriched in common in both undifferentiated ESCs and in cultures differentiated with RA (107). The 5320 genes common among all three cell populations included many "housekeeping" proteins such as clathrin, β and γ actin, Na+/K+ ATPase subunits and 27 different ribosomal proteins; however, comparison with our other enrichment profiles revealed that many of the genes identified as specifically enriched in one or two out of the three cell populations were also included. Thus, a substantial number of these genes may be expressed within all three populations, but show significant up-regulation in one or two out of the three. The Venn diagram in Fig. 3B lists the number of genes enriched in each category but also shows the percentage that is unique to that category. For example, of the 557 genes enriched in cultures differentiated in SFD medium alone, 38.6% were only represented in that category while the remaining 61.4% met the criteria for inclusion in the central pool of 5320 genes expressed to some extent in all three populations. Complete lists of all genes in each category are provided in the Gene Table Supplementary Data File.

Consistent with our evidence for the relative immaturity of cultures induced with SFD medium alone, the genes enriched in this population included many associated with early neural precursors, such as neurogenin1, neurod1, Dlx1, Pax6 and Eomes. In contrast, the list of genes specific to inductions that involved exposure to RA included components of mature neurons, such as synaptic molecules, receptors, channels and neurotransmitters. To visualize these differences in functionality we used Gene Ontology (GO) terms (Ashburner et al., 2000). Fig. 4A highlights GO terms with significant prevalence among genes specifically enriched in SFD medium alone (green), in RA-treated cells (red), or genes enriched in both differentiated cell populations (yellow) relative to ESCs. Genes associated with brain development, neural differentiation, chromatin modification and Wnt receptor signalling were enriched in the cultures differentiated with SFD medium alone, whereas cultures from inductions that had been exposed to RA exhibited a higher proportion of genes associated with mature neurons (ion transport, pre- and post-synaptic membrane, neurotransmitter secretion) (Fig. 4A; Supplementary Tables 3–5).

Profile comparison

To compare our transcriptional profiles quantitatively with previous expression profiling studies we used GOurmet software which allows for platform-independent analysis based on GO terms (Doherty et al., 2006, 2008). Hierarchical clustering revealed that genes specifically enriched in RA-treated cells (RA) cluster with profiles of mature brain tissue (Supplementary Fig. 4) whereas genes specifically enriched in SFD medium alone exhibit the greatest similarity to the profile of E14.5 retinal neuroblasts (Fortunel et al., 2003), a transit-amplifying cell population (Doherty et al., 2008). Inclusion of profiles from non-neuronal cell types further highlights the distinction between stem, transit-amplifying and mature expression patterns. The dendrogram in Fig. 4B illustrates the relationships among 28 different profiled cell populations including 3 profiles of neural stem cells (numbers 17, 18 and 19) and 7 other tissue-derived stem-like populations (numbers 14–16, 20–23), 3 profiles from transit-amplifying cell populations (numbers 25, 27, 28), and 9 profiles from mature tissues (numbers 3, 6–13; see Supplementary materials for complete information on each population profile). In addition to the genes specific to SFD alone and to RA-treated cells, the dendrogram in Fig. 4B also displays lists that include genes upregulated in both of the differentiated cell populations (number 5, SFD vs ES; number 4, RA vs ES) relative to undifferentiated ESCs.

To focus on the differences between cells differentiated with and without RA, we also identified 1366 genes enriched in SFD alone cultures relative to RA-treated cells (number 26, SFD vs RA). These genes, which are likely to be expressed by cells present in the cultures differentiated with SFD alone but absent from RA-treated cultures, were found to cluster most closely with the transit-amplifying populations. In contrast, 1883 genes enriched in RA-treated cultures relative to SFD alone (number 2, RA vs SFD) clustered together with genes that were specific to RA-treated cells (number 1, RA). Taken together, our data suggests that cultures differentiated with SFD medium alone include neurons as well as a substantial representation of cells that are relatively immature and retain a high proliferative capacity, typical of transit-amplifying neuroblasts, whereas cultures induced with a period of exposure to RA are relatively more mature and appear to retain fewer precursor cells.

Cell proliferation

Neural differentiation, both *in vivo* and *in vitro*, requires cells to exit the cell cycle and become postmitotic (Ohnuma and Harris, 2003). Our microarray analysis revealed higher expression of early neural progenitor genes in cultures induced in SFD medium without RA as compared to undifferentiated cells and those induced with exposure to RA. This led us to evaluate the fraction of proliferating cells by incubation with bromodeoxyuridine (BrdU) (Gratzner,

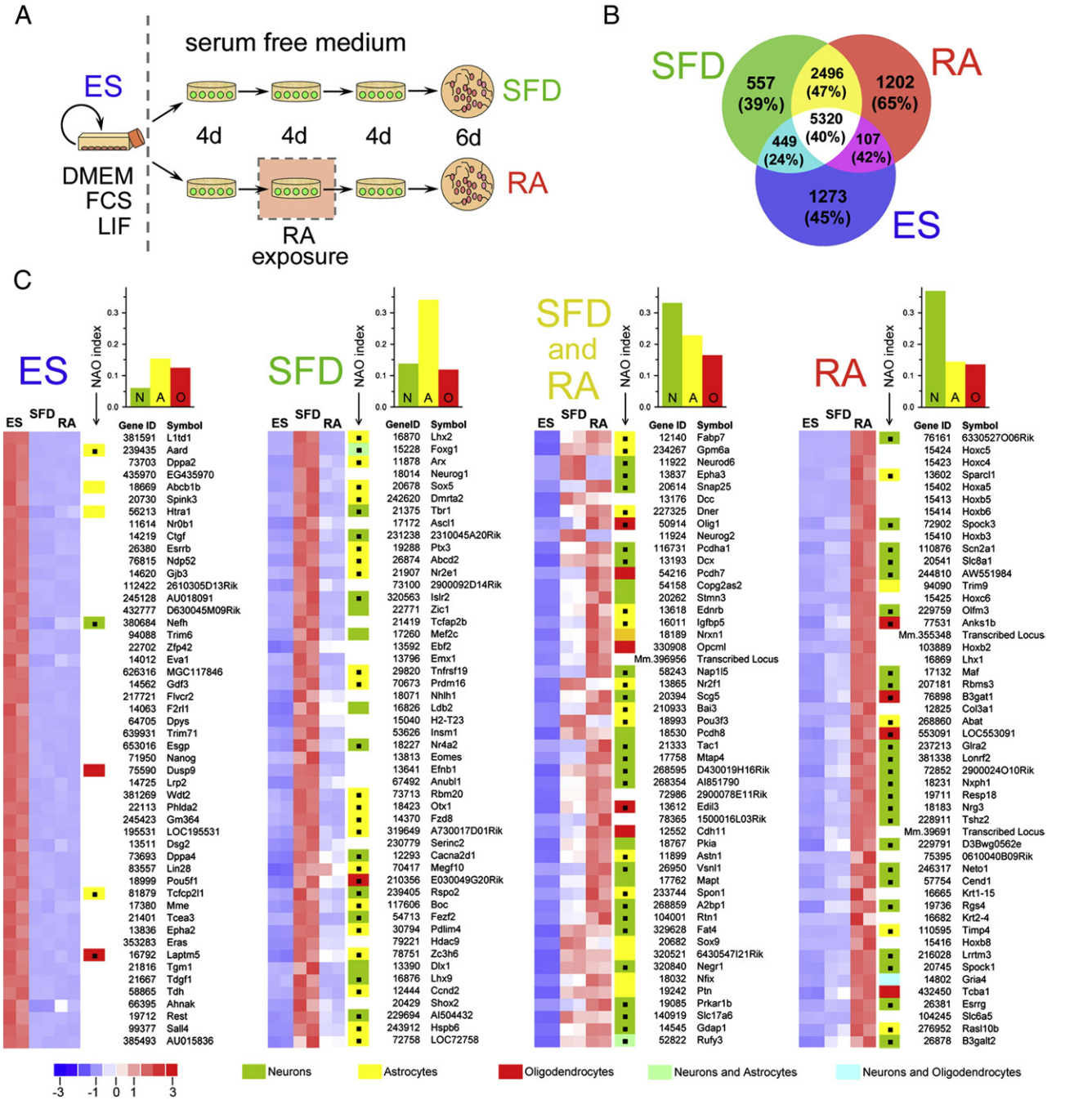

Fig. 3. Transcriptional profiles. (A) Mouse ESCs were maintained in suspension for 12 d in serum free differentiation medium alone (SFD), or with exposure to RA from d4–d8 (RA). mRNA for microarray analysis was prepared from differentiated cells 6 d after plating on laminin plus poly-ornithine, and from feeder-free undifferentiated mouse ESCs (ES) maintained in DMEM plus serum and LIF. (B) Venn diagram showing shared and distinct genes among undifferentiated ESCs (ES, blue), cells induced without RA (SFD, green) and cells induced with exposure to RA (RA, red). (C) Genes specifically enriched in ES, in SFD, in both SFD and RA, and in the RA cell populations. Replicate microarray heat plots for the 50 genes with the highest fold enrichment (lower bound) in each population ordered from highest (top) to lowest (bottom). Genes specifically enriched in neurons (green), astrocytes (yellow), or oligodendrocytes (red) are highlighted. A black dot in the colored box indicates a match with the specific probe set identified by Cahoy et al. (2008) as cell type enriched. Bar plots illustrate a weighted index of cell type-specific expression for all of the genes in each population.

1982). ESC aggregates were maintained for 12 d in SFD medium alone or with addition of RA from d4–d8. Sister cultures received BrdU for periods ranging from 1 to 24 h immediately prior to harvesting at the end of the 12 d induction. Cell aggregates induced with or without RA contained more BrdU positive cells as BrdU exposure time increased; however, the proportion of labelled cells in SFD medium alone was consistently higher than in cultures that had received RA (Figs. 5A–H). After 24 h of BrdU treatment, almost 50% of cells in EBs induced without RA showed positive BrdU signal, whereas only 25% of cells in EBs induced with RA were labelled with BrdU (Fig. 5I). We next compared proliferation on d1–4 after plating by adding BrdU to plated cultures 2 h prior to fixation. Cultures induced with SFD medium alone showed a high proportion of BrdU positive cells (~41%) on d1, and lower proportions on subsequent days. However, cells induced with RA showed much lower BrdU labelling (~5–8%) at all time points (Figs. 5J–L). Collectively, our results suggest that SFD medium alone supports a higher level of continued neural precursor proliferation, whereas exposure to RA promotes exit from the cell cycle and speeds neuronal differentiation and maturation.

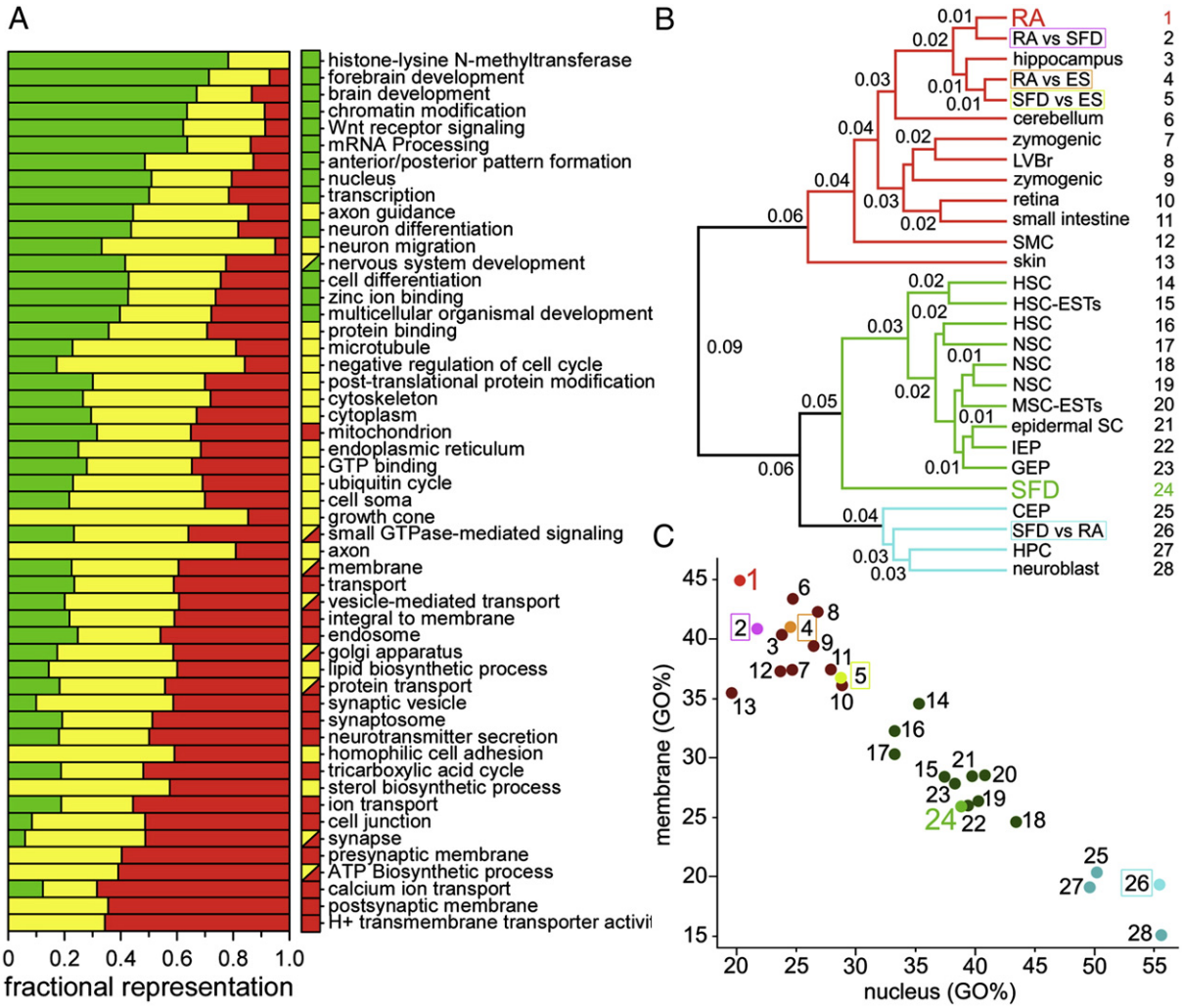

Fig. 4. Profile comparison. (A) Fractional representation of gene sets grouped by Gene Ontology terms. Boxes next to each Gene Ontology term indicate significance for genes specifically enriched in cells induced with SFD medium alone (green), for genes enriched in cells induced with SFD medium plus exposure to RA (red), or genes that were enriched in both populations relative to undifferentiated mES cells (yellow). Note that seven of the Gene Ontology terms (small GTPase-mediated signalling, membrane, vesicle-mediated transport, golgi-apparatus, protein transport, synapse, and ATP biosynthetic process) displayed significant representation both in the RA (red) and in the SFD and RA (yellow) categories, albeit each gene was only assigned to one category (see Supplementary Tables 3–5 for quantitation). (B) Hierarchical clustering based on the relative frequency of Gene Ontology term representation in data sets derived from tissue-derived stem cells, transit amplifying cell types and various differentiated cell populations presented as a dendrogram. Fractional numbers indicate the degree of dissimilarity, calculated as 1-Pearson's coefficient of similarity, between two profiles at the depicted branch point. Genes specifically enriched in cells induced with SFD plus RA exposure (RA, 1) cluster with profiles of mature tissues, including hippocampus (3) and cerebellum (6); whereas genes enriched in the SFD alone cell cultures relative to RA-treated cells (SFD vs RA, 26) clustered most closely with transit-amplifying cell populations (25, 27, 28). Genes specifically enriched in SFD medium alone (SFD, 24) are intermediate to the transit amplifying and tissue-derived stem cell populations. By contrast, genes enriched in RA-treated cells relative to cells differentiated without RA (RA vs SFD, 2) clustered together with the genes specific for RA-treated cells (RA, 1) and with genes enriched in SFD alone (SFD vs ES, 5), or in RA-treated cells (RA vs ES, 4), relative to the undifferentiated ES cells. (C) Segregation of fully differentiated tissues, tissue-specific stem cell populations, and transit amplifying cell types based on fractional representation of membrane and nucleus GO terms.

Neural progenitors

Neurons in the developing CNS are generated from at least three types of progenitor cells, neuroepithelial cells, basal or intermediate progenitors, and radial glial cells, which express different molecular markers, (Doetsch 2003; Goldman, 2003). Neuroepithelial cells express the intermediate filament nestin (Lendahl et al., 1990) and its posttranslational modifications recognized by the antibodies RC1 and RC2 (Malatesta et al., 2003). Radial glia also express nestin as well as the transcription factor Pax6 (Gotz and Barde, 2005; Heins et al., 2002). Unlike neuroepithelial cells and radial glia, basal progenitors express the T box transcription factor Eomes, also known as Tbr2 (Englund et al., 2005). Expression of these progenitor-associated genes persists in proliferative neural precursors in the adult brain (Hodge et al., 2008). Previous studies have highlighted the conversion of ESCs into radial glia (Liour and Yu, 2003; Liour et al., 2006; Bibel et al., 2004; Bouhon et al., 2006), but have not addressed the production of basal progenitors. Our transcriptional profiles indicated that expression of both Pax6 and Tbr2 was significantly up regulated in cells induced with SFD medium alone, although Pax6 (but not Tbr2) was expressed at lower levels in RA-treated cells as well as undifferentiated ESCs.

To visualize the distribution of these progenitor cell markers we performed double immunofluorescence on ESCs induced in SFD medium without or with exposure to RA (Fig. 6). After 12 d in suspension, many cells induced in SFD medium alone expressed only Pax6 (45 ± 5%) or only Tbr2 (13 ± 3%), although a small proportion of cells was found to be immunoreactive for both Pax6 and Tbr2 (10 ± 2%) ($n = 7$; Fig. 6A). Approximately 36 ± 3% of cells induced with exposure to RA expressed Pax6, but Tbr2 was not detected in RA treated cells ($n = 5$; Fig. 6B). At 3 h after plating, cells expressing both nestin and RC2 were observed in cultures induced with RA or without

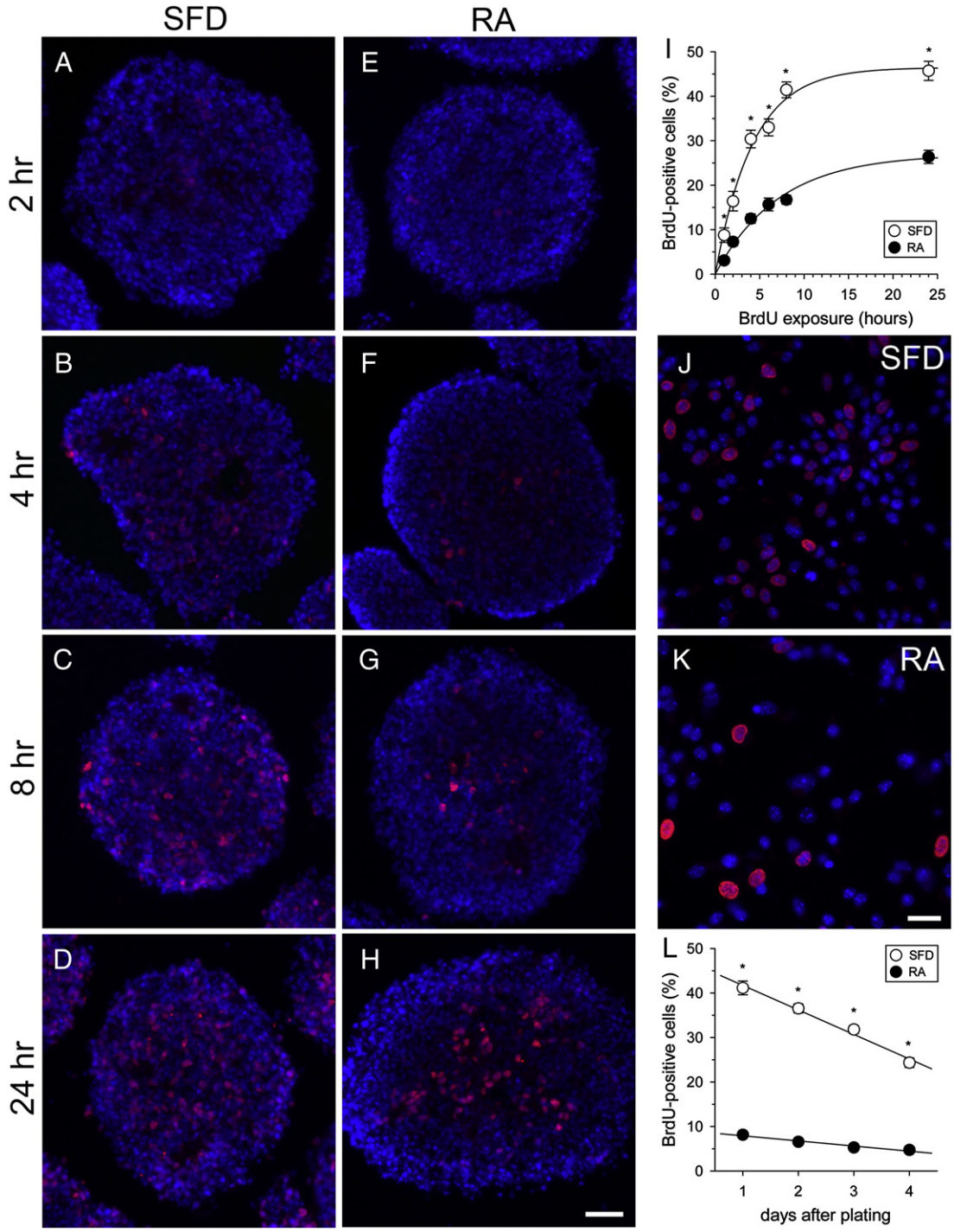

Fig. 5. Cell proliferation. ESC aggregates maintained for 12 d in SFD medium alone (A–D) or with exposure to RA from d4–d8 in suspension (E–H) were incubated with BrdU (20 μg ml^{-1}) for 2 h (A, E); 4 h (B, F); 8 h (C, G) or 24 h (D, H). (I) Percent of Hoechst stained nuclei (blue) in 12 d aggregate cultures that were immunopositive for BrdU (red) plotted as a function of BrdU exposure time. Incorporation of BrdU in dissociated cells 4 d after plating from aggregates maintained 12 d in SFD medium alone (J) or with RA exposure from d4–d8 (K). (L) Percent of immunopositive cells following 2 h incubation with BrdU evaluated in different cultures 1–4 d after plating. Scale bars: 25 μm. Cells exposed to RA displayed lower BrdU labelling both in floating aggregates and in plated cultures, indicating a lower rate of proliferation.

RA (Figs. 6C, D). Pax6 also was expressed in cells induced with RA or without RA, and many of the Pax6-positive cells coexpressed vimentin or RC2 (Figs. 6E–H). Tbr2 immunofluorescence was observed only by cells induced in SFD medium without RA, and some of the Tbr2-positive cells were immunoreactive for vimentin or RC2 (Supplementary Figs. 5A, B). Furthermore, the neural precursor population displaying strong vimentin immuno-fluorescence was distinct from neurons labelled with antibodies to β-3-tubulin (Supplementary Fig. 5C). Together, these data suggest that exposure to RA alters the specification of neural precursors, blocking the production of basal progenitors.

Neuronal phenotype specification

Previous work suggests that exposure to RA can promote caudalization and suppress rostral neural structures (Maden, 2007;

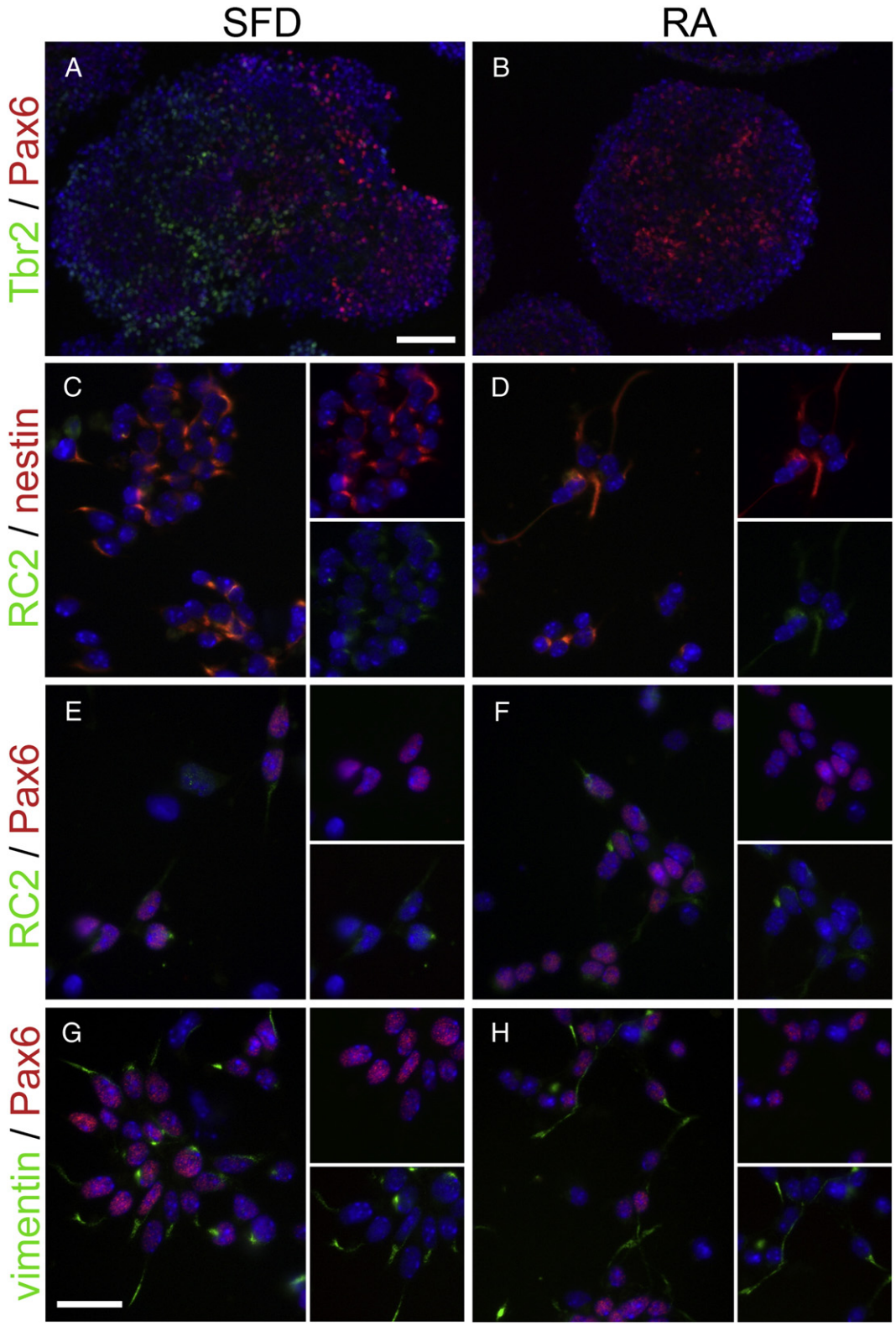

Fig. 6. Neural progenitors. ESC aggregates maintained for 12 d in SFD medium alone (A) contained cells immunopositive for Pax6 (red), a marker expressed in radial glia, or for Tbr2 (green), which is expressed in basal progenitor cells. In contrast, RA-treated aggregates lacked Tbr2-positive cells (B). Scale bar: 50 μm. (C–H) After dissociation, plating, and 3 h in culture, numerous cells induced without (C, E, G) or with (D, F, H) exposure to RA were co-labelled with antibodies to RC2 and nestin (C, D), or with Pax6 and RC2 (E, F) or vimentin (G, H), suggesting that the majority of Pax6-positive cells are likely to be radial glia. Scale bar: 25 μm.

Wichterle et al., 2002; Bouhon et al., 2006). To infer the positional identity of differentiated ESC, we compared our upregulated gene lists with a spatial database of gene expression from the mouse genome informatics (MGI) website, which contains comprehensive information about expression patterns (Smith et al., 2007). As illustrated in Fig. 7, genes expressed in telencephalon, diencephalon and mesencephalon were more prevalent in cells differentiated in SFD medium alone relative to cultures treated with RA (Fig. 7A), whereas genes

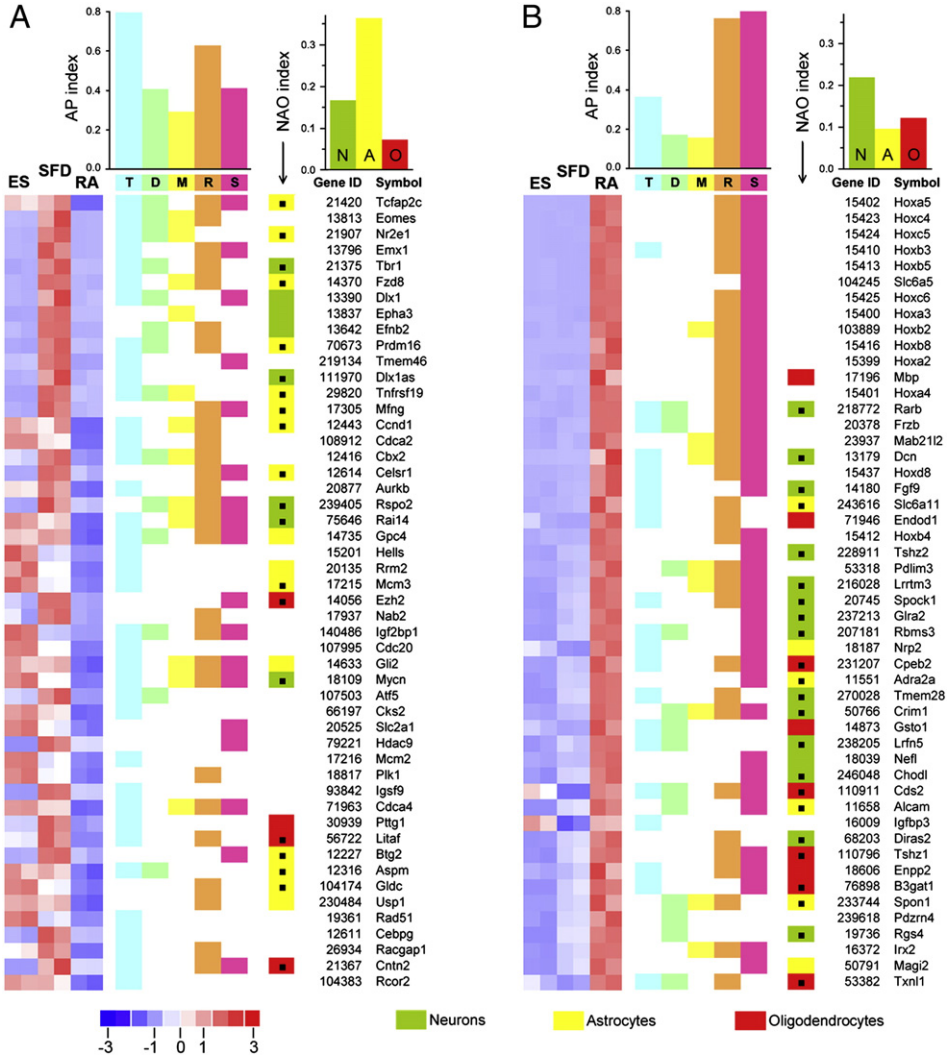

Fig. 7. Positional identity. (A) Replicate microarray heat plots for the 50 genes with differential anatomical expression patterns that showed the highest fold enrichment (lower bound) in cells differentiated in SFD medium alone relative to differentiation with exposure to RA, and (B) the 50 genes with differential anatomical expression that were most enriched in RA-treated cells relative to cells induced with SFD medium alone. Genes expressed in telencephalon (T, blue), diencephalon (D, green), mesencephalon (M, yellow), rhombencephalon (R, orange), and spinal cord (S, rose) in the mouse genome informatics anatomical expression database are indicated. Bar plots illustrate a weighted index of gene expression for each anterior–posterior (AP) anatomical domain. The AP index distributions were significantly different for genes enriched in the two differentiated cell populations (Chi-square, $p<0.0001$). T, D and M genes were enriched in cells induced with SFD medium alone, whereas R and S genes were enriched in cells differentiated with exposure to RA (z-test comparison of proportions, $p\leq0.023$). Genes specifically enriched in neurons (N, green), astrocytes (A, yellow), or oligodendrocytes (O, red) are highlighted. Plots show a weighted index of cell type-specific expression for all of the genes in each population, which were significantly different in (A) and (B) (Chi-square, $p=0.0007$). Genes expressed in astrocytes were enriched in cells differentiated with SFD medium alone (z-test comparison of proportions, $p<0.001$).

expressed in rhombencephalon and spinal cord predominated in cells differentiated with RA exposure (Fig. 7B). Interestingly, genes involved with regulating transcription were among the transcripts most highly enriched in each cell population (Figs. 7A, B).

To gain further insight into the positional identity of ESCs induced with RA or without RA we used antibodies to transcription factors associated with the differentiation of specific neuronal populations. In cultures induced with SFD medium for 10–12 d followed by 4 d adherent culture, 35 ± 3% of cells coexpressed β-3-tubulin and Tbr1 (Fig. 8A), a transcription factor expressed in the dorsal telencephalon (pallium) (Hevner et al., 2001; Remedios et al., 2007) and restricted to glutamatergic neurons (Hevner et al., 2001). Accordingly, nearly all cells that strongly expressed the vesicular glutamate transporter1 (VGLUT1), were positive for Tbr1 (Fig. 8B) whereas GABAergic neurons, expressing glutamic acid decarboxylase (GAD), were uniformly negative for Tbr1 (Fig. 8C). Instead, many of the GAD-positive neurons expressed Islet1 (Fig. 8C), which is a LIM homeodomain transcription factor expressed in the spinal cord and ventral regions of the telencephalon, diencephalon, mesencephalon, and rhombencephalon (Ericson et al., 1995; Pfaff et al., 1996). Islet1-positive cells become motorneurons in mesencephalon, rhombencephalon and spinal cord (Pfaff et al., 1996; Simon et al., 1994) but not in telencephalon and diencephalon (Ericson et al., 1995). In cultures induced with SFD medium alone, 30 ± 3% of β-3-tubulin-positive cells expressed Islet1 and over 80% of cells immunopositive for Islet1 and β-3-tubulin also expressed GAD (Fig. 8C), which is prevalent in the subpallium/ventral telencephalon (Muzio et al., 2002; Yun et al., 2001). Diencephalic Islet1-positive neurons can be distinguished from telencephalic Islet1-positive neurons by their expression of LIM homeodomain transcription factor, Lim1 (Ericson et al., 1995; Fotaki et al., 2006). In the cultures differentiated with SFD medium alone, approximately 20% of cells were immunopositive for Lim1/2; however, none of the Islet1-positive neurons was co-labelled for Lim1 (Supplementary Fig. 6). These data suggest that Islet1-positive neurons in cultures differentiated with SFD medium alone acquire ventral telencephalic identity in the absence of RA. A

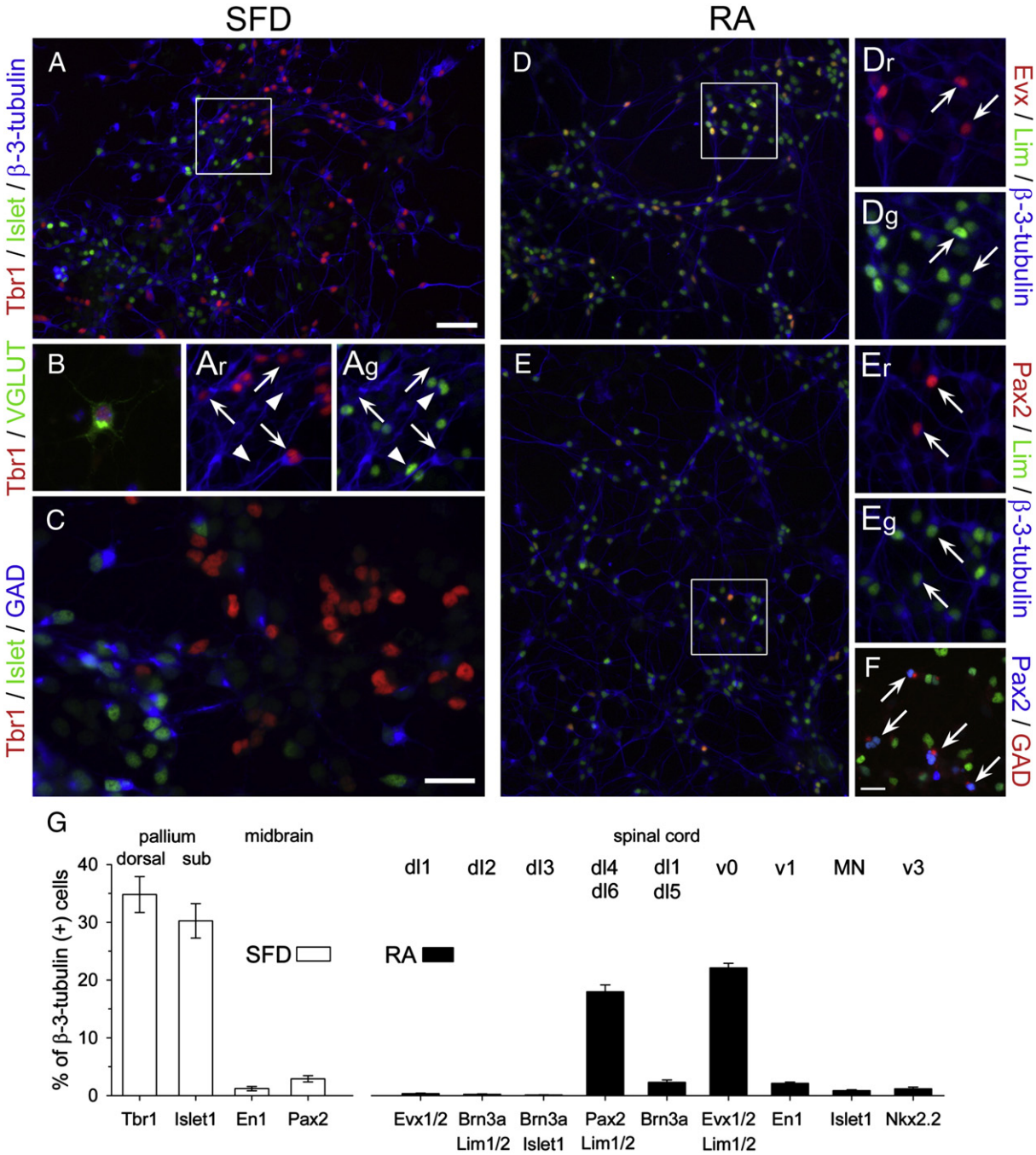

Fig. 8. Neuronal phenotype specification. (A–C) In plated cultures differentiated with SFD medium alone, distinct β-3-tubulin-positive (blue) neuron populations were immunolabelled with the dorsal pallial marker Tbr1 (Ar, arrows, red) or with the subpallial marker Islet1 (Ag, arrowheads, green). Scale bar: 50 μm. (B) Cells strongly immunopositive for the glutamatergic marker VGLUT1 (green) were co-labelled with Tbr1 (red), (C) whereas GAD-positive GABAergic cells (blue) co-labelled with Islet1 (green), but not Tbr1 (red). Scale bar: 25 μm. (D–F) In plated cultures differentiated with brief exposure to RA, ~22% β-3-tubulin-positive neurons (blue) co-labelled with Evx1/2 (red) and Lim1/2 (green) (Dr and Dg, arrows), markers for V0 ventral spinal neurons, whereas ~18% co-expressed markers of dI4 and dI6 dorsal spinal neurons Pax2 (red) and Lim1/2 (green) (Er and Eg, arrows). (F) Most Pax2-positive (blue) neurons were co-labelled for GAD (red) as well as Lim1/2 (green). Scale bar: 25 μm. (G) Quantitation of immunopositive cells differentiated with SFD medium alone (open bars), or with exposure to RA (solid bars); 21–35 fields each condition, 462 ± 13 cells/field. The dorsal pallial marker Tbr1 and subpallial marker Islet1 together account for ~65% of all β-3-tubulin-positive neurons in SFD alone cultures. In cultures prepared from RA-treated aggregates, ~40% of β-3-tubulin-positive neurons co-labelled with Pax2 and Lim1/2 typical of dI4/dI6 neurons, or with Evx1/2 and Lim1/2 characteristic of V0 neurons.

few cells in cultures induced with SFD medium alone expressed Pax2 (3 ± 0.5%) or Engrail1 (1 ± 0.4%) which are typical markers for midbrain (Davis and Joyner, 1988; Matsunaga et al., 2000), whereas no cells were found to be positive for Hoxb4, a marker for the caudal hindbrain and spinal cord (Graham et al., 1988; Nordstrom et al., 2006) (Supplementary Fig. 7).

In contrast to differentiation with SFD medium alone, which led cells to adopt anterior phenotypes, in cultures induced with exposure to RA, almost 90% of β-3-tubulin positive cells were immunopositive for Hoxb4 (Supplementary Fig. 7), consistent with acquisition of caudal positional identity for the hindbrain or spinal cord (Gould et al., 1997; Nordstrom et al., 2006). To investigate subtype identity of neurons produced following exposure to RA, we used antibodies to transcription factors with regionally restricted expression patterns along the dorsoventral axis of the spinal cord (Briscoe et al., 2000; Helms and Johnson, 2003). Evx1/2 is expressed in specific dorsal (dI1)

and ventral (V0) interneuron populations (Briscoe et al., 2000; Pierani et al., 1999) that can be distinguished by co-expression of Lim1/2 in ventral Evx1/2-positive cells (Pierani et al., 1999), whereas intervening dorsal interneuron populations (dI4, dI5) co-express Pax2 and Lim1/2 (Gross et al., 2002). Among β-3-tubulin positive cells induced in SFD medium with exposure to RA, 22 ± 0.8% were positive for both Evx1/2 and Lim1/2 (Fig. 8D arrows), suggesting that they acquired V0 fate; 18 ± 1.2% expressed both Pax2 and Lim1/2, but not Evx1/2 (Fig. 8E arrows), suggesting that they are dI4 or dI6 neurons. In the developing spinal cord, dorsal Pax2-positive neurons are GABAergic (Cheng et al., 2004). Most Pax2-positive, Lim1/2-positive neurons derived from ESCs with exposure to RA expressed the GABAergic neuronal marker, GAD (Fig. 8F arrows). A few β-3-tubulin-positive cells (~10%) were immunopositive for transcription factors that are expressed by dorsal interneuron subtype dI1 (Evx1) (Pierani et al., 1999) or dI2 (Brn3a and Lim1/2) (Muller et al., 2002), or ventral interneuron subtype V1 (En1) (Ericson et al., 1997; Matise and Joyner, 1997), V3 (Nkx2.2) (Briscoe et al., 1999), or motorneurons (Islet1) (Pfaff et al., 1996) (Fig. 8G). Together, these data suggest that a large proportion of neurons (~60–70%) induced with SFD medium alone acquire anterior neuronal identity, whereas neurons induced with exposure to RA express molecular markers with regionally restricted expression patterns in the spinal cord (Supplementary Fig. 8).

Discussion

We have demonstrated efficient neural conversion of mouse ESCs using serum- and retinoid-free differentiation (SFD) medium that contains few exogenous proteins and have used this system to compare the molecular and phenotypic properties of cells induced to differentiate with or without exposure to RA. Treatment with RA promotes neural maturation and alters the proportion of neurons expressing specific phenotypic properties, such as GABA production or glycine receptor subunit expression. Our microarray analysis identified a large number of neural genes that are expressed by cells that differentiate from mouse ESCs whether or not they are treated with RA. In addition, our results showed that cultures induced with SFD medium alone are selectively enriched in genes involved in early neurogenesis, whereas cultures induced with RA are enriched for genes associated with mature neurons. Together with our BrdU labelling studies, these results demonstrate that SFD medium permits the differentiation of neurons but also supports the continued proliferation of neural precursors, whereas exposure to RA restricts precursor proliferation and promotes maturation. Our results further suggest that cells induced with SFD medium alone acquire anterior neural identity whereas cultures induced in SFD medium with brief exposure to RA adopt posterior neural identity.

RA and neural differentiation

In serum-containing cultures, RA is essential to induce efficient neural differentiation from ESCs (Bain et al., 1995, 1996; Glaser and Brüstle, 2005; Rohwedel et al., 1999). Previous studies suggest that neural differentiation can proceed without RA under serum-free conditions (Okabe et al., 1996; Wiles and Johansson, 1999; Finley et al., 1999; Tropepe et al., 2001; Ying et al., 2003; Watanabe et al., 2005; Bouhon et al., 2005), although the use of proprietary media and supplements makes it difficult to rule out a cryptic retinoid inducer in many studies. Importantly, recent work suggests that ESCs cultured in PBS alone for 4 h attain neural identity as indicated by expression of Sox1 and nestin (Smukler et al., 2006). However, ESCs induced in PBS without any exogenous factors underwent massive cell death. We have demonstrated that our SFD medium devoid of exogenous proteins, aside from insulin, transferrin and BSA, supports neural conversion of ESCs without compromising cell growth and survival.

Consistently, our experiments indicate that cells differentiated with brief exposure to RA lose stem cell identity, adopt neural fate, and acquire mature axonal/dendritic polarity more rapidly than cells induced with SFD medium alone. Previous work suggests that RA promotes neural differentiation by inducing proneural genes, such as Sox1, Sox6, Brn2 and neurogenin1, and suppressing antineural genes (Maden, 2007). For example, a major component of ESC neuralization by RA is thought to involve the induction of Wnt signalling inhibitors, secreted frizzled-related protein 2 (Sfrp2) and dickkopf homolog 1 (Dkk1) (Aubert et al., 2002; Verani et al., 2007; Watanabe et al., 2005). Our gene expression profiles indicate that Sfrp2 is up regulated in cells induced in SFD medium with or without exposure to RA. In addition, Sox6, Brn2 and neurogenin2 are all upregulated in cells differentiated in SFD medium regardless of exposure to RA and the inhibitor of Wnt and FGF signalling pathways Tmem46, also known as Shisa2 (Furushima et al., 2007), is selectively enriched in cultures differentiated in SFD medium without RA.

The relative maturity of ESCs differentiated with exposure to RA may reflect the conversion of neural progenitor cells to postmitotic neurons. Thus, neurons induced with exposure to RA undergo their final mitosis at an earlier time point than cells induced with SFD medium alone. We also observe, however, that although neurons induced with SFD medium alone are less mature than those differentiated with RA during the first few days in adherent culture, they gradually become mature in longer-term culture, suggesting that they will eventually "catch up" with the level of maturity attained by RA treated cells. Another possibility, which we cannot exclude, is that RA directly induces genes associated with neuronal maturation or with the mature state. During neurogenesis, after exiting the cell cycle, young neurons initiate formation and outgrowth of neurites that ultimately become axons and dendrites. Studies in cell culture, have shown that treatment with RA increases neurite outgrowth from a variety of central and peripheral neurons (Clagett-Dame et al., 2006). Therefore, it is possible that exposure to RA speeds the acquisition of polarity as a secondary effect to the promotion of neurite formation.

Proliferation vs differentiation

Mouse ESCs divide rapidly and without apparent limit *in vitro* (Suda et al., 1987), but division rate decreases under conditions promoting differentiation (Stead et al., 2002). Cell proliferation and differentiation are tightly coordinated by cell cycle controls involving the formation of complexes between cyclins and cyclin-dependent kinases (CDKs), a process inhibited by cyclin-dependant kinase inhibitors (CKIs) (Burdon et al., 2002). RA promotes differentiation and inhibits cell proliferation by inducing cell cycle arrest in a variety of different embryonic cells including ESCs (Lin et al., 2005). Within 72 h of RA treatment, mouse ESCs express the tumor suppressor gene *p53*, reducing expression of *Nanog*, one of the genes required for maintenance of pluripotency, and increase expression of *p21*, the CKI gene that enhances ESC differentiation (Lin et al., 2005). Our cultures, whether induced with or without exposure to RA, showed reduced expression of cyclin E1 that is highly active in undifferentiated ESCs (Stead et al., 2002) and showed increased expression of cyclin-dependent kinase inhibitors 1B (p27) and 2D (p19), which independently inhibit cell cycle progression in the CNS. Cultures induced with SFD alone showed increased expression of cyclin D2 and Cdk4, which together form a complex that is found in neural precursors and is increased upon initiation of ESC differentiation (Savatier et al., 1996). Our results show that cultures induced with or without RA include postmitotic neurons and proliferating cells; however, cultures induced with SFD alone exhibit more proliferation. Thus, RA mediated suppression of cyclin genes and induction of CKI genes are likely to be one mechanism by which RA accelerates cell cycle exit and promotes ESC neural differentiation.

Positional and phenotypic identity

Nieuwkoop proposed that neurons are initially specified as forebrain but can become gradually posteriorized by caudalizing signals (Nieuwkoop, 1952). Our data suggests that a large proportion of ESCs induced in SFD medium alone exhibits forebrain identity, but that brief exposure to RA results in acquisition of features characteristic of hindbrain and spinal cord, consistent with the Nieuwkoop model. Another recent study (Gaspard et al., 2008) supports the proposal that serum-free ESC differentiation yields predominantly telencephalic identity (see also Bouhon et al. (2006)), with ventral GABAergic differentiation being dependent on autocrine sonic hedgehog signalling (Gaspard et al., 2008). In contrast, other serum-free conditions involving proprietary media were reported to result in a high percentage of ESC-derived neurons adopting midbrain identity (Kawasaki et al., 2000), with efficiency of telencephalic differentiation being enhanced by exogenous addition of the Wnt antagonist Dkk1 (Watanabe et al., 2005), suggesting that the baseline conditions may include unknown caudalizing factors that must be suppressed or overcome for acquisition of more anterior neural phenotypes.

RA suppresses expression of anterior genes and causes caudalization of neural tissues *in vivo* (Maden, 2007). Consistent with this, our results show that genes highly expressed in hindbrain and spinal cord, including 14 members of the Hox gene family (Nolte and Krumlauf, 2007), are enriched in cultures induced with exposure to RA, whereas genes prevalent in more anterior structures were lacking. For example, Tbr2, which is highly expressed in basal progenitors of dorsal forebrain (Englund et al., 2005), was dramatically enriched in cells differentiated in SFD medium alone relative to cells that were exposed to RA, whereas both differentiated cell populations express molecular markers for neuroepithelial and radial glial cells that generate neurons both in the cortex and in spinal cord (Malatesta et al., 2003). Moreover, a substantial proportion of cells induced with exposure to RA exhibited transcription factor expression patterns that were consistent with spinal cord identity. Dorso-ventral patterning in spinal cord depends on RA and gradients of sonic hedgehog, which specifies ventral phenotypes, and of bone morphogenetic protein (BMP) family members, originating from the roof plate, that promote dorsal phenotypes (Jessell, 2000). Importantly, about 40% of mES cells induced with exposure to RA expressed transcription factors characteristic of V0 or of dI6 cell populations that lie adjacent to each other midway between the dorsal and ventral extremes *in vivo* (Supplementary Fig. 8). Approximately ~22% co-expressed Evx1 and Lim1/2 (V0), whereas 18% expressed Pax2 and Lim1/2 together with GAD (dI4 and dI6), suggesting that specification of caudal neuronal subtypes by RA parallels that observed *in vivo* (see also Wichterle et al. (2002)). In contrast to this interpretation, Bibel et al. (2004) suggested that selection of highly proliferating ESCs followed by aggregation in serum-containing medium and exposure to RA yielded radial glia that differentiated into cells with physiological and morphological characteristics of glutamatergic neurons from cerebral cortex. However, when we induced ESCs in serum containing medium with exposure to RA, although most of the neurons were glutamatergic (Finley et al., 1996), many cells expressed the caudal marker Hoxb4 while none expressed the cortical cell marker Tbr1 that is prevalent with induction in SFD medium in the absence of RA (Supplementary Fig. 7). Thus, it seems likely that RA caudalizes differentiating ESCs regardless the presence or absence of serum, or selection for rapidly dividing cells.

Our study shows that SFD culture medium induces robust neural conversion of ESCs and efficient specification of anterior neural fate, and reproduces the *in vivo* effect of RA on neural differentiation. Development of methods for reprogramming somatic cells has opened up the possibility of generating customized patient-specific stem cells that can be used for tissue repair and cell replacement (Park et al., 2008). Maximizing the therapeutic potential of stem cells will require identifying conditions that allow for efficient commitment to particular cell phenotypes. Previous studies have shown that ESCs can differentiate into specific neural types by sequential exposure to extracellular matrix proteins (Goetz et al., 2006) and signalling molecules (Salero and Hatten, 2007; Wichterle et al., 2002) associated with their development *in vivo*. The restricted number of identified ingredients in SFD medium should aid in efforts to elucidate the signals necessary for differentiation of additional neural cell types.

Acknowledgments

This study is supported by grants from the NIH (NS045023 and NS30888, JEH; DK079798, JCM; GM39746, RWM). We are grateful to Tim Wilding and Aileen Lu for their technical assistance and to David Gottlieb, Paul Gray and Kristen Kroll for their helpful comments on the manuscript. We thank the Alvin J. Siteman Cancer Center at Washington University School of Medicine and Barnes-Jewish Hospital in St. Louis, Mo., for the use of the Multiplexed Gene Analysis Core. The Siteman Cancer Center is supported in part by an NCI Cancer Center Support Grant #P30 CA91842.

Appendix A. Supplementary data

Supplementary data associated with this article can be found, in the online version, at doi:10.1016/j.ydbio.2009.02.001.

References

Adams, L.D., Choi, L., Xian, H.Q., Yang, A., Sauer, B., Wei, L., Gottlieb, D.I., 2003. Double lox targeting for neural cell transgenesis. Mol. Brain Res. 110, 220–233.

Akagi, H., Hirai, K., Hishinuma, F., 1991. Cloning of a glycine receptor subtype expressed in rat brain and spinal cord during a specific period of neuronal development. FEBS Lett. 281, 160–166.

Ashburner, M., Ball, C.A., Blake, J.A., Botstein, D., Butler, H., Cherry, J.M., Davis, A.P., Dolinski, K., Dwight, S.S., Eppig, J.T., Harris, M.A., Hill, D.P., Issel-Tarver, L., Kasarskis, A., Lewis, S., Matese, J.C., Richardson, J.E., Ringwald, M., Rubin, G.M., Sherlock, G., 2000. Gene ontology: tool for the unification of biology. Nat. Genet. 25, 25–29.

Aubert, J., Dunstan, H., Chambers, I., Smith, A., 2002. Functional gene screening in embryonic stem cells implicates Wnt antagonism in neural differentiation. Nat. Biotechnol. 20, 1240–1245.

Bain, G., Kitchens, D., Yao, M., Huettner, J.E., Gottlieb, D.I., 1995. Embryonic stem cells express neuronal properties *in vitro*. Dev. Biol. 168, 342–357.

Bain, G., Ray, W.J., Yao, M., Gottlieb, D.I., 1996. Retinoic acid promotes neural and represses mesodermal gene expression in mouse embryonic stem cells in culture. Biochem. Biophys. Res. Commun. 223, 691–694.

Barberi, T., Klivenyi, P., Calingasan, N.Y., Lee, H., Kawamata, H., Loonam, K., Perrier, A.L., Bruses, J., Rubio, M.E., Topf, N., Tabar, V., Harrison, N.L., Beal, M.F., Moore, M.A., Studer, L., 2003. Neural subtype specification of fertilization and nuclear transfer embryonic stem cells and application in parkinsonian mice. Nat. Biotechnol. 21, 1200–1207.

Bellochio, E.E., Reimer, R.J., Fremeau, R.T., Edwards, R.H., 2000. Uptake of glutamate into synaptic vesicles by an inorganic phosphate transporter. Science 289, 957–960.

Bibel, M., Richter, J., Schrenk, K., Tucker, K.L., Staiger, V., Korte, M., Goetz, M., Barde, Y.A., 2004. Differentiation of mouse embryonic stem cells into a defined neuronal lineage. Nat. Neurosci. 7, 1003–1009.

Bouhon, I.A., Kato, H., Chandran, S., Allen, N.D., 2005. Neural differentiation of mouse embryonic stem cells in chemically defined medium. Brain Res. Bull. 68, 62–75.

Bouhon, I.A., Joannides, A., Kato, H., Chandran, S., Allen, N.D., 2006. Embryonic stem cell-derived neural progenitors display temporal restriction to neural patterning. Stem Cells 24, 1908–1913.

Brewer, G.J., Torricelli, J.R., Everge, E.K., Price, P.J., 1993. Optimized survival of hippocampal neurons in B27-supplemented neurobasal, a new serum-free medium combination. J. Neurosci. Res. 35, 567–576.

Briscoe, J., Pierani, A., Jessell, T.M., Ericson, J., 2000. A homeodomain protein code specifies progenitor cell identity and neuronal fate in the ventral neural tube. Cell 101, 435–445.

Briscoe, J., Sussel, L., Serup, P., Hartigan-O'Connor, D., Jessell, T.M., Rubenstein, J.L.R., Ericson, J., 1999. Homeobox gene Nkx2.2 and specification of neuronal identity by graded Sonic hedgehog signalling. Nature 398, 622–627.

Brüstle, O., Jones, K.N., Learish, R.D., Karram, K., Choudhary, K., Wiestler, O.D., Duncan, I.D., McKay, R.D., 1999. Embryonic stem cell-derived glial precursors: a source of myelinating transplants. Science 285, 754–756.

Burdon, T., Smith, A., Savatier, P., 2002. Signalling, cell cycle and pluripotency in embryonic stem cells. Trends Cell Biol. 12, 432–438.

Caccamo, D., Katsetos, C.D., Herman, M.M., Frankfurter, A., Collins, V.P., Rubinstein, L.J., 1989. Immunohistochemistry of a spontaneous murine ovarian teratoma with neuroepithelial differentiation. Neuron-associated beta-tubulin as a marker for primitive neuroepithelium. Lab. Invest. 60, 390–398.

Caceres, A., Banker, G.A., Binder, L., 1986. Immunocytochemical localization of tubulin and microtubule-associated protein 2 during the development of hippocampal neurons in culture. J. Neurosci. 6, 714–722.
Cahoy, J.D., Emery, B., Kaushal, A., Foo, L.C., Zamanian, J.L., Christopherson, K.S., Xing, Y., Lubischer, J.L., Krieg, P.A., Krupenko, S.A., Thompson, W.J., Barres, B.A., 2008. A transcriptome database for astrocytes, neurons, and oligodendrocytes: a new resource for understanding brain development and function. J. Neurosci. 28, 264–278.
Cai, C., Grabel, L., 2007. Directing the differentiation of embryonic stem cells to neural stem cells. Dev. Dyn. 236, 3255–3266.
Chang, Y.C., Gottlieb, D.I., 1988. Characterization of the proteins purified with monoclonal antibodies to glutamic acid decarboxylase. J. Neurosci. 8, 2123–2130.
Cheng, L., Arata, A., Mizuguchi, R., Qian, Y., Karunaratne, A., Gray, P.A., Arata, S., Shirasawa, S., Bouchard, M., Luo, P., Chen, C.L., Busslinger, M., Goulding, M., Onimaru, H., Ma, Q., 2004. Tlx3 and Tlx1 are post-mitotic selector genes determining glutamatergic over GABAergic cell fates. Nat. Neurosci. 7, 510–517.
Clagett-Dame, M., McNeill, E.M., Muley, P.D., 2006. Role of all-*trans* retinoic acid in neurite outgrowth and axonal elongation. J. Neurobiol. 66, 739–756.
Davis, C.A., Joyner, A.L., 1988. Expression patterns of the homeo box-containing genes En-1 and En-2 and the proto-oncogene int-1 diverge during mouse development. Genes Dev. 2, 1736–1744.
Doetsch, F., 2003. The glial identity of neural stem cells. Nat. Neurosci. 6, 1127–1134.
Doetschman, T.C., Eistetter, H., Katz, M., Schmidt, W., Kemler, R., 1985. The *in vitro* development of blastocyst-derived embryonic stem cell lines: formation of visceral yolk sac, blood islands and myocardium. J. Embryol. Exp. Morphol. 87, 27–45.
Doherty, J.M., Carmichael, L.K., Mills, J.C., 2006. GOurmet: a tool for quantitative comparison and visualization of gene expression profiles based on gene ontology (GO) distributions. BMC Bioinformatics 7, 151.
Doherty, J.M., Geske, M.J., Stappenbeck, T.S., Mills, J.C., 2008. Diverse adult stem cells share specific higher-order patterns of gene expression. Stem Cells 26, 2124–2130.
Dotti, C.G., Sullivan, C.A., Banker, G.A., 1988. The establishment of polarity by hippocampal neurons in culture. J. Neurosci. 8, 1454–1468.
Englund, C., Fink, A., Lau, C., Pham, D., Daza, R.A., Bulfone, A., Kowalczyk, T., Hevner, R.F., 2005. Pax6, Tbr2, and Tbr1 are expressed sequentially by radial glia, intermediate progenitor cells, and postmitotic neurons in developing neocortex. J. Neurosci. 25, 247–251.
Ericson, J., Muhr, J., Placzek, M., Lints, T., Jessell, T.M., Edlund, T., 1995. Sonic hedgehog induces the differentiation of ventral forebrain neurons: a common signal for ventral patterning within the neural tube. Cell 81, 747–756.
Ericson, J., Rashbass, P., Schedl, A., Brenner-Morton, S., Kawakami, A., van Heyningen, V., Jessell, T.M., Briscoe, J., 1997. Pax6 controls progenitor cell identity and neuronal fate in response to graded Shh signaling. Cell 90, 169–180.
Finley, M.F.A., Kulkarni, N., Huettner, J.E., 1996. Synapse formation and establishment of neuronal polarity by P19 embryonic carcinoma cells and embryonic stem cells. J. Neurosci. 16, 1056–1065.
Finley, M.F.A., Devata, S., Huettner, J.E., 1999. BMP-4 inhibits neural differentiation in murine embryonic stem cells. J. Neurobiol. 40, 271–287.
Fortunel, N.O., Otu, H.H., Ng, H.H., Chen, J., Mu, X., Chevassut, T., Li, X., Joseph, M., Bailey, C., Hatzfeld, J.A., Hatzfeld, A., Usta, F., Vega, V.B., Long, P.M., Libermann, T.A., Lim, B., 2003. Comment on "'Stemness': transcriptional profiling of embryonic and adult stem cells" and "a stem cell molecular signature". Science. 302, 393.
Fotaki, V., Yu, T., Zaki, P.A., Mason, J.O., Price, D.J., 2006. Abnormal positioning of diencephalic cell types in neocortical tissue in the dorsal telencephalon of mice lacking functional Gli3. J. Neurosci. 26, 9282–9292.
Fraichard, A., Chassande, O., Bilbaut, G., Dehay, C., Savatier, P., Samarut, J., 1995. *In vitro* differentiation of embryonic stem cells into glial cells and functional neurons. J. Cell Sci. 108, 3181–3188.
Furushima, K., Yamamoto, A., Nagano, T., Shibata, M., Miyachi, H., Abe, T., Ohshima, N., Kiyonari, H., Aizawa, S., 2007. Mouse homologues of Shisa antagonistic to Wnt and Fgf signalings. Dev. Biol. 306, 480–492.
Gaspard, N., Bouschet, T., Hourez, R., Dimidschstein, J., Naeije, G., van den Ameele, J., Espuny-Camacho, I., Herpoel, A., Passante, L., Schiffmann, S.N., Gaillard, A., Vanderhaeghen, P., 2008. An intrinsic mechanism of corticogenesis from embryonic stem cells. Nature 455, 351–357.
Glaser, T., Brüstle, O., 2005. Retinoic acid induction of ES-cell-derived neurons: the radial glia connection. Trends Neurosci. 28, 397–400.
Goetz, A.K., Scheffler, B., Chen, H.X., Wang, S., Suslov, O., Xiang, H., Brüstle, O., Roper, S.N., Steindler, D.A., 2006. Temporally restricted substrate interactions direct fate and specification of neural precursors derived from embryonic stem cells. Proc. Natl. Acad. Sci. U. S. A. 103, 11063–11068.
Goldman, S., 2003. Glia as neural progenitor cells. Trends Neurosci. 26, 590–596.
Gould, A., Morrison, A., Sproat, G., White, R.A., Krumlauf, R., 1997. Positive cross-regulation and enhancer sharing: two mechanisms for specifying overlapping Hox expression patterns. Genes Dev. 11, 900–913.
Gotz, M., Barde, Y.A., 2005. Radial glial cells defined and major intermediates between embryonic stem cells and CNS neurons. Neuron 46, 369–372.
Graham, A., Papalopulu, N., Lorimer, J., McVey, J.H., Tuddenham, E.G., Krumlauf, R., 1988. Characterization of a murine homeo box gene, Hox-2.6, related to the *Drosophila* deformed gene. Genes Dev. 2, 1424–1438.
Gratzner, H.G., 1982. Monoclonal antibody to 5-bromo- and 5-iododeoxyuridine: a new reagent for detection of DNA replication. Science 218, 474–475.
Gross, M.K., Dottori, M., Goulding, M., 2002. Lbx1 specifies somatosensory association interneurons in the dorsal spinal cord. Neuron 34, 535–549.
Hadjantonakis, A.K., Gertsenstein, M., Ikawa, M., Okabe, M., Nagy, A., 1998. Generating green fluorescent mice by germline transmission of green fluorescent ES cells. Mech. Dev. 76, 79–90.
Harvey, R.J., Schmieden, V., Von Holst, A., Laube, B., Rohrer, H., Betz, H., 2000. Glycine receptors containing the alpha4 subunit in the embryonic sympathetic nervous system, spinal cord and male genital ridge. Eur. J. Neurosci. 12, 994–1001.
Heins, N., Malatesta, P., Cecconi, F., Nakafuku, M., Tucker, K.L., Hack, M.A., Chapouton, P., Barde, Y.A., Gotz, M., 2002. Glial cells generate neurons: the role of the transcription factor Pax6. Nat. Neurosci. 5, 308–315.
Helms, A.W., Johnson, J.E., 2003. Specification of dorsal spinal cord interneurons. Curr. Opin. Neurobiol. 13, 42–49.
Hevner, R.F., Shi, L., Justice, N., Hsueh, Y., Sheng, M., Smiga, S., Bulfone, A., Goffinet, A.M., Campagnoni, A.T., Rubenstein, J.L., 2001. Tbr1 regulates differentiation of the preplate and layer 6. Neuron 29, 353–366.
Hodge, R.D., Kowalczyk, T.D., Wolf, S.A., Encinas, J.M., Rippey, C., Enikolopov, G., Kempermann, G., Hevner, R.F., 2008. Intermediate progenitors in adult hippocampal neurogenesis: Tbr2 expression and coordinate regulation of neuronal output. J. Neurosci. 28, 3707–3717.
Jessell, T.M., 2000. Neuronal specification in the spinal cord: inductive signals and transcriptional codes. Nat. Rev. Genet. 1, 20–29.
Kawasaki, H., Mizuseki, K., Nishikawa, S., Kaneko, S., Kuwana, Y., Nakanishi, S., Nishikawa, S.I., Sasai, Y., 2000. Induction of midbrain dopaminergic neurons from ES cells by stromal cell-derived inducing activity. Neuron 28, 31–40.
Kuhse, J., Laube, B., Magalei, D., Betz, H., 1993. Assembly of the inhibitory glycine receptor: identification of amino acid sequence motifs governing subunit stoichiometry. Neuron 11, 1049–1056.
Lee, S.H., Lumelsky, N., Studer, L., Auerbach, J.M., McKay, R.D., 2000. Efficient generation of midbrain and hindbrain neurons from mouse embryonic stem cells. Nat. Biotechnol. 18, 675–679.
Lendahl, U., Zimmerman, L.B., McKay, R.D., 1990. CNS stem cells express a new class of intermediate filament protein. Cell 60, 585–595.
Li, C., Wong, W.H., 2001. Model-based analysis of oligonucleotide arrays: expression index computation and outlier detection. Proc. Natl. Acad. Sci. U. S. A. 98, 31–36.
Lin, T., Chao, C., Saito, S.I., Mazur, S.J., Murphy, M.E., Appella, E., Xu, Y., 2005. p53 induces differentiation of mouse embryonic stem cells by suppressing Nanog expression. Nat. Cell Biol. 7, 165–171.
Liour, S.S., Yu, R.K., 2003. Differentiation of radial glia-like cells from embryonic stem cells. Glia 42, 109–117.
Liour, S.S., Kraemer, S.A., Dinkins, M.B., Su, C.Y., Yanagisawa, M., Yu, R.K., 2006. Further characterization of embryonic stem cell-derived radial glial cells. Glia 53, 43–56.
Liu, S., Qu, Y., Stewart, T.J., Howard, M.J., Chakrabortty, S., Holekamp, T.F., McDonald, J.W., 2000. Embryonic stem cells differentiate into oligodendrocytes and myelinate in culture and after spinal cord transplantation. Proc. Natl. Acad. Sci. U. S. A. 97, 6126–6131.
Maden, M., 2007. Retinoic acid in the development, regeneration and maintenance of the nervous system. Nat. Rev. Neurosci. 8, 755–765.
Malatesta, P., Hack, M.A., Hartfuss, E., Kettenmann, H., Klinkert, W., Kirchhoff, F., Gotz, M., 2003. Neuronal or glial progeny: regional differences in radial glia fate. Neuron 37, 751–764.
Matise, M.P., Joyner, A.L., 1997. Expression patterns of developmental control genes in normal and Engrailed-1 mutant mouse spinal cord reveal early diversity in developing interneurons. J. Neurosci. 17, 7805–7816.
Matsunaga, E., Araki, I., Nakamura, H., 2000. Pax6 defines the di-mesencephalic boundary by repressing En1 and Pax2. Development 127, 2357–2365.
Malosio, M.L., Marqueze-Pouey, B., Kuhse, J., Betz, H., 1991. Widespread expression of glycine receptor subunit mRNAs in the adult and developing rat brain. EMBO J. 10, 2401–2409.
Muller, T., Brohmann, H., Pierani, A., Heppenstall, P.A., Lewin, G.R., Jessell, T.M., Birchmeier, C., 2002. The homeodomain factor Lbx1 distinguishes two major programs of neuronal differentiation in the dorsal spinal cord. Neuron 34, 551–562.
Murry, C.E., Keller, G., 2008. Differentiation of embryonic stem cells to clinically relevant populations: lessons from embryonic development. Cell 132, 661–680.
Muzio, L., DiBenedetto, B., Stoykova, A., Boncinelli, E., Gruss, P., Mallamaci, A., 2002. Conversion of cerebral cortex into basal ganglia in Emx2(−/−) Pax6(Sey/Sey) double-mutant mice. Nat. Neurosci. 5, 737–745.
Newcomb, R., Sun, X., Taylor, L., Curthoys, N., Giffard, R.G., 1997. Increased production of extracellular glutamate by the mitochondrial glutaminase following neuronal death. J. Biol. Chem. 272, 11276–11282.
Nieuwkoop, P.D., 1952. Activation and organization of the central nervous system in amphibians. J. Exp. Zool. 120, 1–108.
Nolte, C., Krumlauf, R., 2007. Expression of Hox genes in the nervous system of vertebrates. In: Papageorgiou, S. (Ed.), Hox Gene Expression. Springer, New York, pp. 14–41.
Niwa, H., Miyazaki, J., Smith, A.G., 2000. Quantitative expression of Oct-3/4 defines differentiation, dedifferentiation or self-renewal of ES cells. Nat. Genet. 24, 372–376.
Nordstrom, U., Maier, E., Jessell, T.M., Edlund, T., 2006. An early role for WNT signaling in specifying neural patterns of Cdx and Hox gene expression and motor neuron subtype identity. PLoS Biol. 4, e252.
Okabe, S., Forsberg-Nilsson, K., Spiro, A.C., Segal, M., McKay, R.D., 1996. Development of neuronal precursor cells and functional postmitotic neurons from embryonic stem cells *in vitro*. Mech. Dev. 59, 89–102.
Ohnuma, S., Harris, W.A., 2003. Neurogenesis and the cell cycle. Neuron 40, 199–208.
Park, I.H., Zhao, R., West, J.A., Yabuuchi, A., Huo, H., Ince, T.A., Lerou, P.H., Lensch, M.W., Daley, G.Q., 2008. Reprogramming of human somatic cells to pluripotency with defined factors. Nature 451, 135–136.
Pfaff, S.L., Mendelsohn, M., Stewart, C.L., Edlund, T., Jessell, T.M., 1996. Requirement for LIM homeobox gene Isl1 in motor neuron generation reveals a motor neuron-dependent step in interneuron differentiation. Cell 84, 309–320.

Piechotta, K., Weth, F., Harvey, R.J., Friauf, E., 2001. Localization of rat glycine receptor alpha1 and alpha2 subunit transcripts in the developing auditory brainstem. J. Comp. Neurol. 438, 336–352.

Pierani, A., Brenner-Morton, S., Chiang, C., Jessell, T.M., 1999. A sonic hedgehog-independent, retinoid-activated pathway of neurogenesis in the ventral spinal cord. Cell 97, 903–915.

Ramalho-Santos, M., Yoon, S., Matsuzaki, Y., Mulligan, R.C., Melton, D.A., 2002. "Stemness": transcriptional profiling of embryonic and adult stem cells. Science 298, 597–600.

Remedios, R., Huilgol, D., Saha, B., Hari, P., Bhatnagar, L., Kowalczyk, T., Hevner, R.F., Suda, Y., Aizawa, S., Ohshima, T., Stoykova, A., Tole, S., 2007. A stream of cells migrating from the caudal telencephalon reveals a link between the amygdala and neocortex. Nat. Neurosci. 10, 1141–1150.

Rohwedel, J., Guan, K., Wobus, A.M., 1999. Induction of cellular differentiation by retinoic acid *in vitro*. Cells Tiss. Org. 165, 190–202.

Salero, E., Hatten, M.E., 2007. Differentiation of ES cells into cerebellar neurons. Proc. Natl. Acad. Sci. U. S. A. 104, 2997–3002.

Savatier, P., Lapillonne, H., van Grunsven, L.A., Rudkin, B.B., Samarut, J., 1996. Withdrawal of differentiation inhibitory activity/leukemia inhibitory factor up-regulates D-type cyclins and cyclin-dependent kinase inhibitors in mouse embryonic stem cells. Oncogene 12, 309–322.

Simon, H., Guthrie, S., Lumsden, A., 1994. Regulation of SC1/DM-GRASP during the migration of motor neurons in the chick embryo brain stem. J. Neurobiol. 25, 1129–1143.

Smith, C.M., Finger, J.H., Hayamizu, T.F., McCright, I.J., Eppig, J.T., Kadin, J.A., Richardson, J.E., Ringwald, M., 2007. The mouse gene expression database (GXD): 2007 update. Nucleic Acids Res. 35, D618–D623.

Smukler, S.R., Runciman, S.B., Xu, S., van der Kooy, D., 2006. Embryonic stem cells assume a primitive neural stem cell fate in the absence of extrinsic influences. J. Cell Biol. 172, 79–90.

Stead, E., White, J., Faast, R., Conn, S., Goldstone, S., Rathjen, J., Dhingra, U., Rathjen, P., Walker, D., Dalton, S., 2002. Pluripotent cell division cycles are driven by ectopic Cdk2, cyclin A/E and E2F activities. Oncogene 21, 8320–8333.

Strübing, C., Ahnert-Hilger, G., Shan, J., Wiedenmann, B., Hescheler, J., Wobus, A.M., 1995. Differentiation of pluripotent embryonic stem cells into the neuronal lineage *in vitro* gives rise to mature inhibitory and excitatory neurons. Mech. Dev. 53, 275–287.

Suda, Y., Suzuki, M., Ikawa, Y., Aizawa, S., 1987. Mouse embryonic stem cells exhibit indefinite proliferative potential. J. Cell. Physiol. 133, 197–201.

Takahashi, K., Tanabe, K., Ohnuki, M., Narita, M., Ichisaka, T., Tomoda, K., Yamanaka, S., 2007. Induction of pluripotent stem cells from adult human fibroblasts by defined factors. Cell 131, 861–872.

Takamori, S., Rhee, J.S., Rosenmund, C., Jahn, R., 2000. Identification of a vesicular glutamate transporter that defines a glutamatergic phenotype in neurons. Nature 407, 189–194.

Thomson, J.A., Itskovitz-Eldor, J., Shapiro, S.S., Waknitz, M.A., Swiergiel, J.J., Marshall, V.S., Jones, J.M., 1998. Embryonic stem cell lines derived from human blastocysts. Science 282, 1145–1147.

Tropepe, V., Hitoshi, S., Sirard, C., Mak, T.W., Rossant, J., van der Kooy, D., 2001. Direct neural fate specification from embryonic stem cells: a primitive mammalian neural stem cell stage acquired through a default mechanism. Neuron 30, 65–78.

Verani, R., Cappuccio, I., Spinsanti, P., Gradini, R., Caruso, A., Magnotti, M.C., Motolese, M., Nicoletti, F., Melchiorri, D., 2007. Expression of the Wnt inhibitor Dickkopf-1 is required for the induction of neural markers in mouse embryonic stem cells differentiating in response to retinoic acid. J. Neurochem. 100, 242–250.

Watanabe, K., Kamiya, D., Nishiyama, A., Katayama, T., Nozaki, S., Kawasaki, H., Watanabe, Y., Mizuseki, K., Sasai, Y., 2005. Directed differentiation of telencephalic precursors from embryonic stem cells. Nat. Neurosci. 8, 288–296.

Wichterle, H., Lieberam, I., Porter, J.A., Jessell, T.M., 2002. Directed differentiation of embryonic stem cells into motor neurons. Cell 110, 385–397.

Wiles, M.V., Johansson, B.M., 1999. Embryonic stem cell development in a chemically defined medium. Exp. Cell Res. 247, 241–248.

Ying, Q.L., Stavridis, M., Griffiths, D., Li, M., Smith, A., 2003. Conversion of embryonic stem cells into neuroectodermal precursors in adherent monoculture. Nat. Biotechnol. 21, 183–186.

Yun, K., Potter, S., Rubenstein, J.L., 2001. Gsh2 and Pax6 play complementary roles in dorsoventral patterning of the mammalian telencephalon. Development 128, 193–205.

SUPPLEMENTARY MATERIALS

SUPPLEMENTARY FIGURES

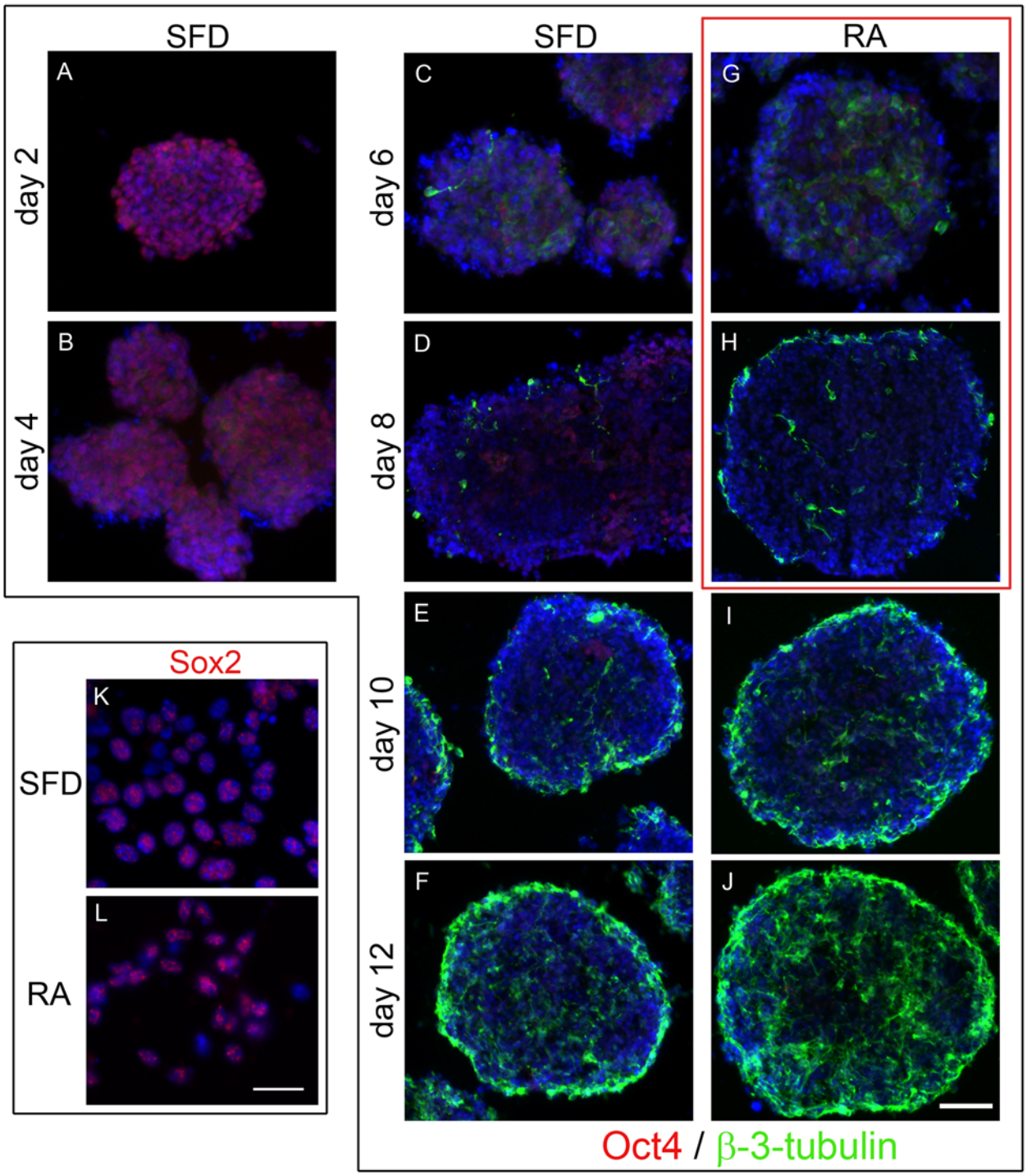

Figure S1 – RA Accelerates Neural Differentiation

EBs formed in SFD medium without RA were fixed after 2d (A), 4d (B), 6d (C, G), 8d (D, H), 10d (E, I) or 12d (F, J). One set was maintained in SFD medium alone (A-F), another set received RA from d4-d8 in suspension (G-J). Expression of Oct3/4 (*red*), a marker for undifferentiated ES cells, declined over the first 4d. Expression of the neuron-specific β-3-tubulin (*green*) increased gradually in SFD medium without RA but more rapidly in cultures with RA exposure. Hoechst33342 (*blue*). Scale bar: 50 µm. (K, L) Immunofluorescence for Sox2 (*red*), a transcription factor expressed in ESCs and differentiating neural cells [Li et al., 1998; Conti et al., 2005], in cell nuclei 2d after plating in cells differentiated with SFD medium alone (K), or with exposure to RA (L). Hoechst33342 (*blue*). Scale bar: 20 µm.

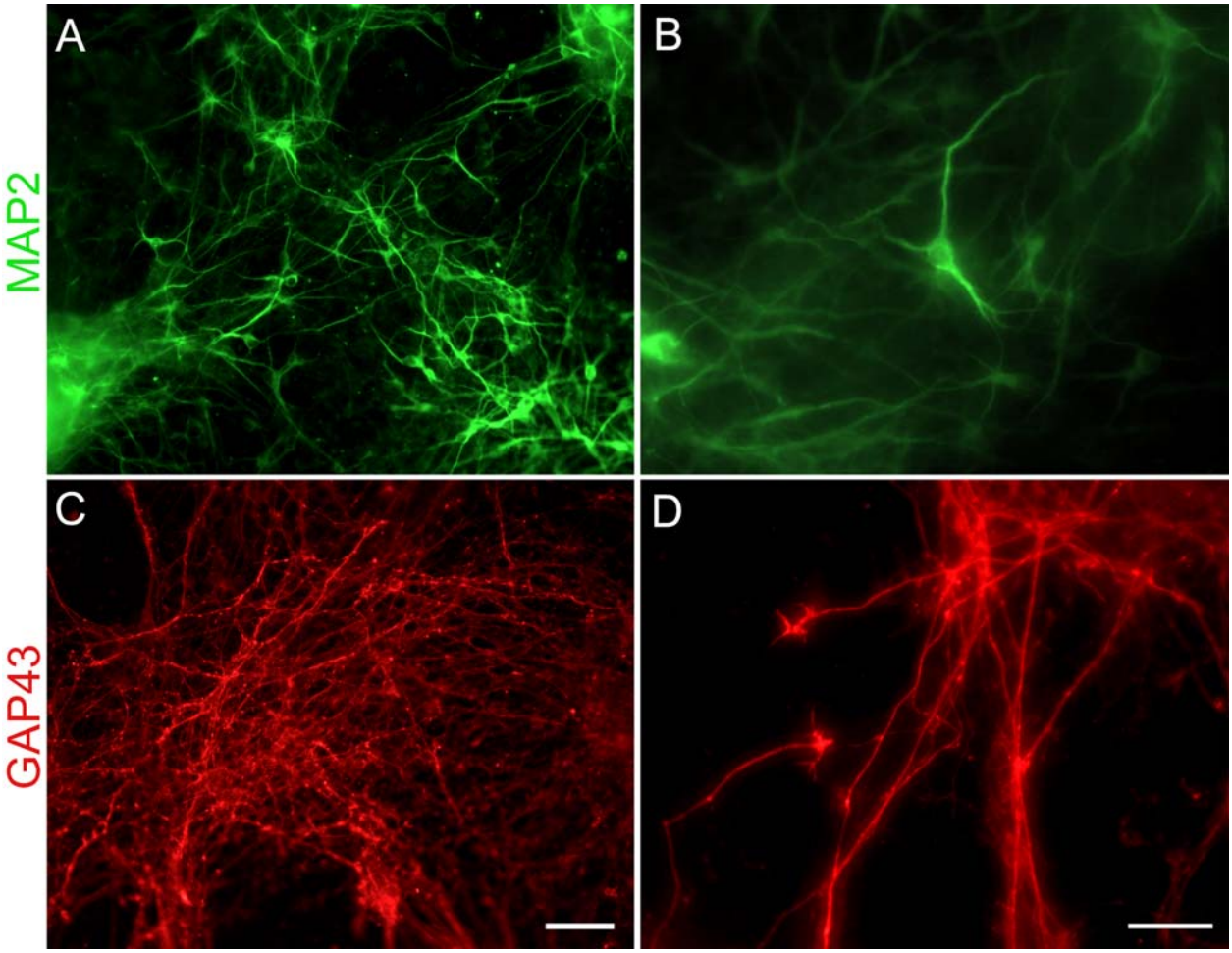

Figure S2 – Neuronal Polarity Established in Mature Cultures Differentiated without RA.

MAP2 immunofluorescence (A, B, *green*) and GAP43 immunofluorescence (C, D, *red*) 12d after plating cells dissociated from ESC aggregates maintained in SFD medium for 12d. Scale Bar: 50 µm (A, C); 25 µm (B, D).

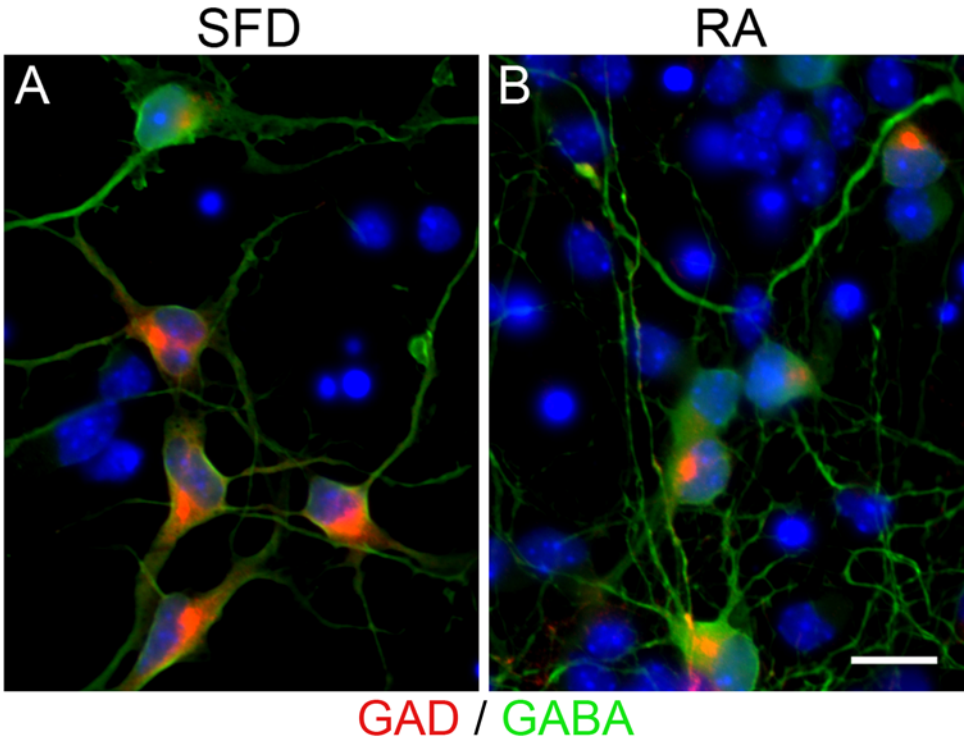

Figure S3 – Coexpression of GABA and GAD.

Co-localization of GAD (*red*) and GABA (*green*) in cells differentiated in SFD medium alone (A) or with exposure to RA (B). Hoechst33342 (*blue*). Scale Bar: 15 µm.

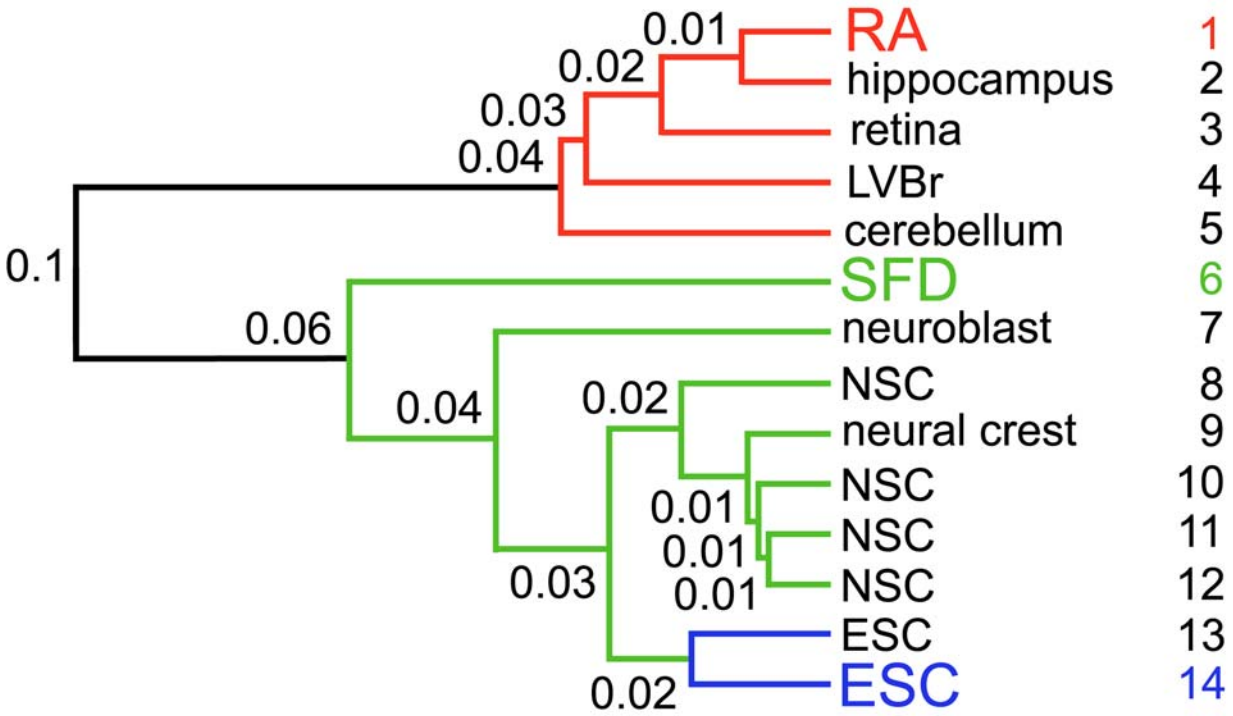

Figure S4 – Dendrogram of Neural Subtypes and Precursors.

Hierarchical clustering based on the relative frequency of Gene Ontology term representation in data sets derived from stem cells and various differentiated cell populations presented as a dendrogram. Fractional numbers indicate the degree of dissimilarity, calculated as 1-Pearson's coefficient of similarity, between two profiles at the depicted branch point. Genes specific to cells induced with SFD plus RA exposure (RA, 1) cluster with profiles of mature brain tissues (2-5), whereas genes specific to cells induced with SFD medium alone (SFD, 6) are most similar to neuroblasts from E14.5 mouse retina (7) and more weakly related to neural stem cell populations derived from cultured neurospheres (NSC, 8, 10-12). Genes specific to our undifferentiated mouse ESCs (ESC, 14) cluster with a previously defined ESC profile (13).

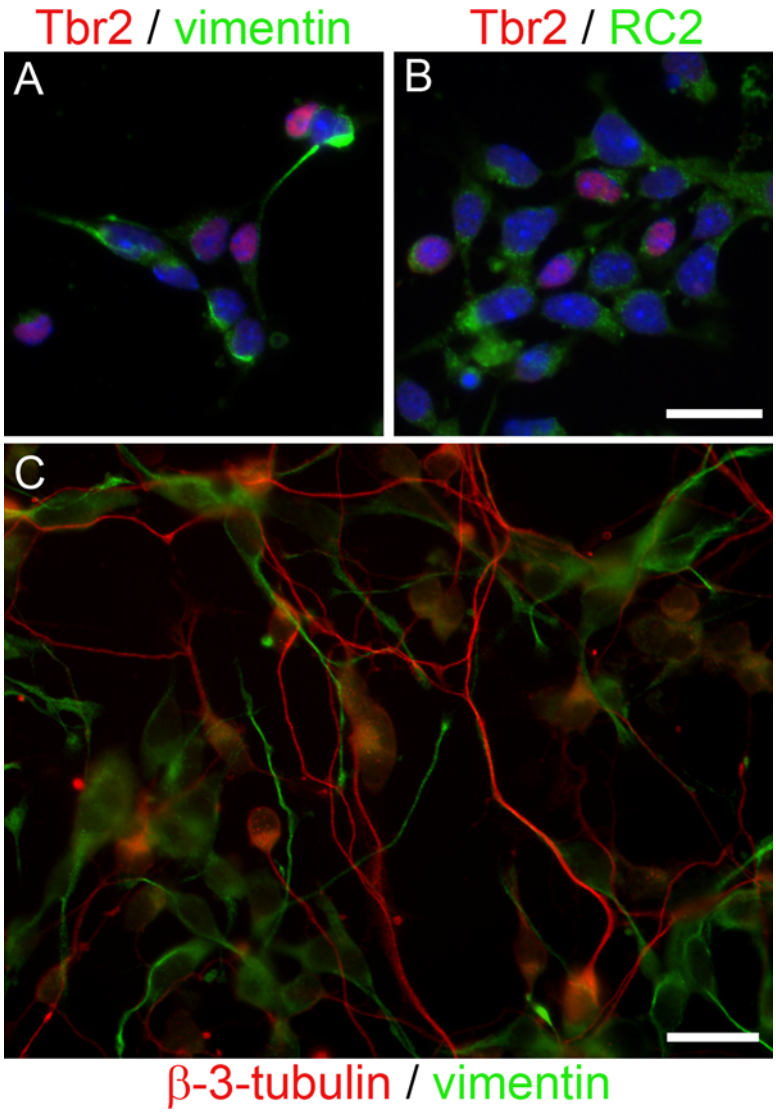

Figure S5 – Vimentin Immunofluorescence in Neural Precursors differentiated in SFD medium without RA.

In cultures 3h after plating, nuclear Tbr2 immunofluorescence (*red*) in cells immunopositive for vimentin (A, *green*) or RC2 (B, *green*). Hoechst33342 (*blue*). (C) Neural precursor cells immunofluorescent for vimentin (*green*) were distinct from β-3-tubulin-positive neurons (*red*), 2d in culture. Scale Bars: 25 µm.

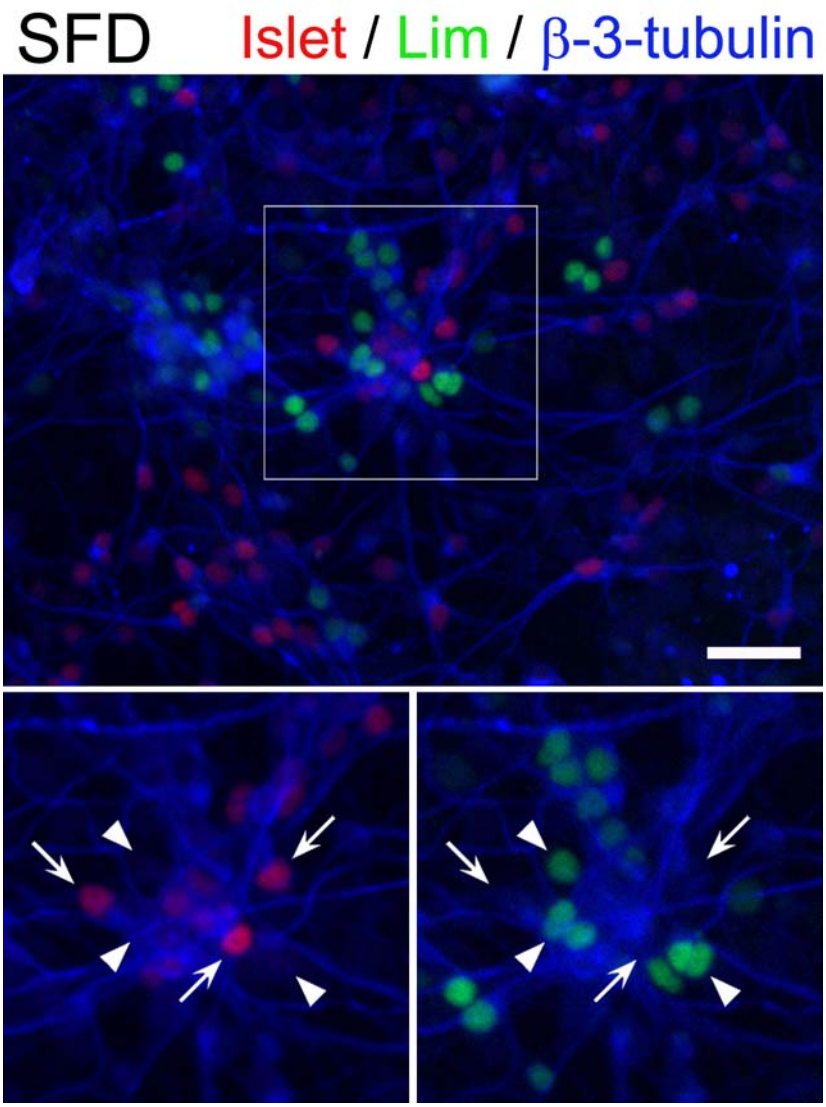

Figure S6 – Distinct neural populations express Islet1 and Lim1/2.

Nuclear immuno-fluorescence for Islet1 (*red, arrows*) and Lim1/2 (*green, arrowheads*) was segregated to different β-3-tubulin-positive (*blue*) neuron populations in cultures differentiated in SFD medium without RA, 4d after plating. Scale Bar: 50 µm.

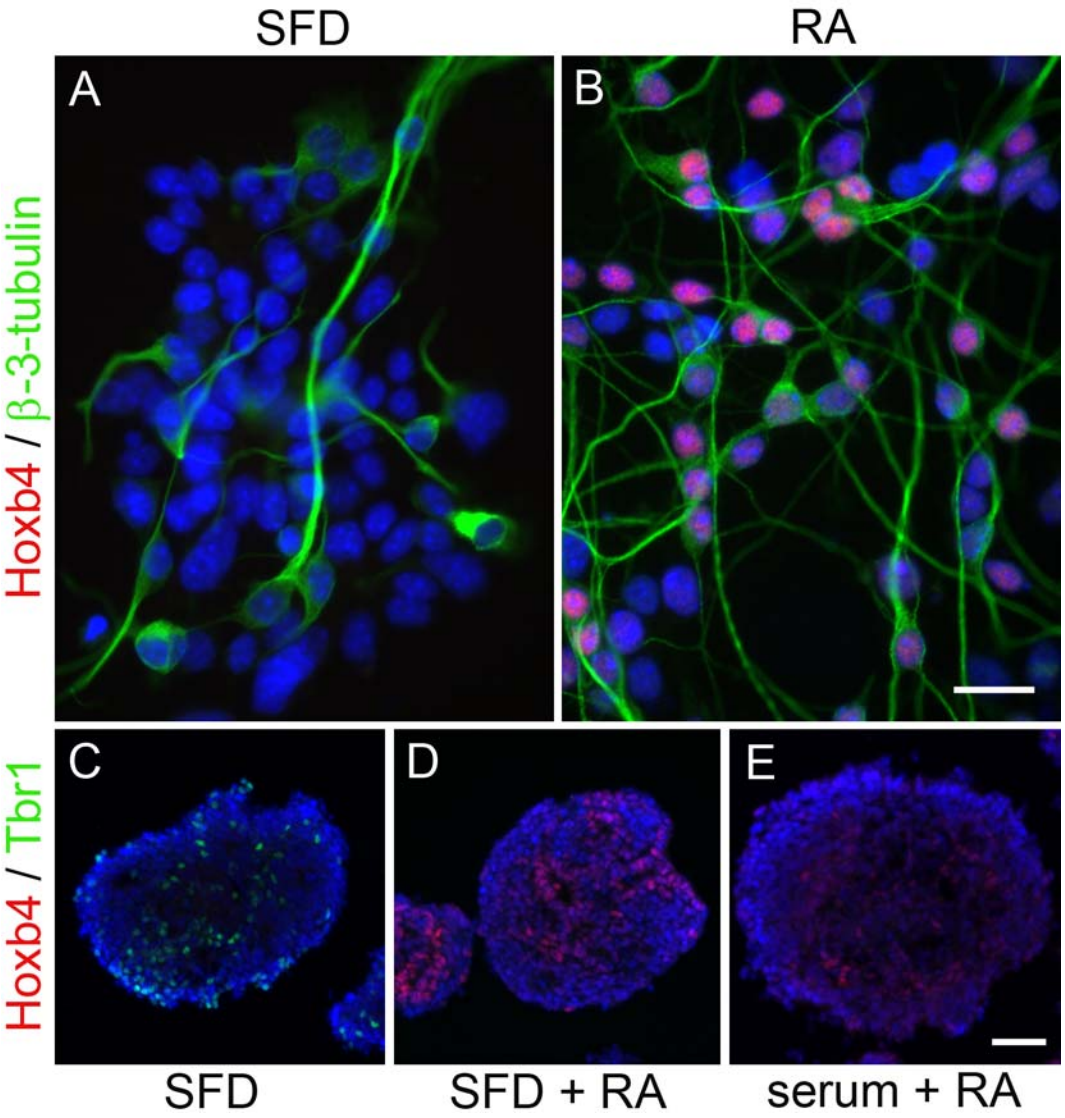

Figure S7 – Differentiation with exposure to RA promotes caudal identity.

Nuclear Hoxb4 immunofluorescence (*red*) was absent from cells differentiated in SFD medium alone (A), but present in the nuclei of most cells from aggregates that had received RA (B). Neurons visualized with anti-β-3-tubulin (*green*); Hoechst33342 (*blue*). Scale Bar: 20 µm. (C-E) Immuno-fluorescence for Tbr1 (*green*) and Hoxb4 (*red*) in sections of aggregates cultured in SFD medium alone (C), SFD medium plus treatment with RA d4-d8 (D), or in DMEM plus 20% calf serum with exposure to RA d4-d8 (E). Hoechst33342 (*blue*). Scale Bar: 50 µm.

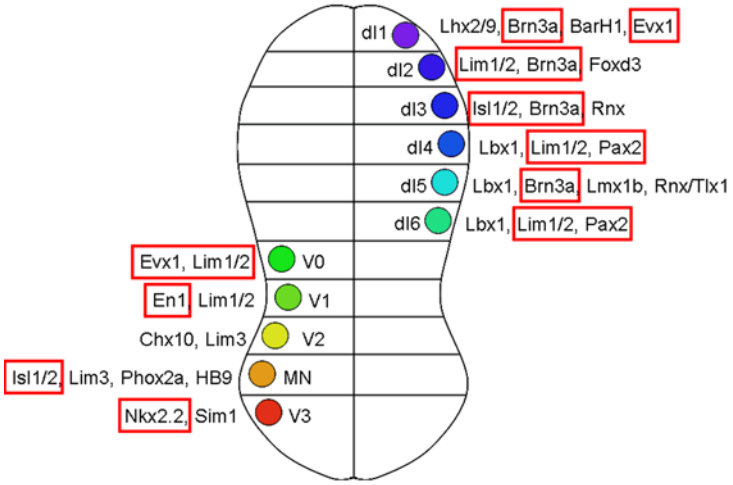

Figure S8 – Schematic Spinal Cord Cross Section.

Molecular markers that delineate specific dorsal (right) and ventral (left) progenitor domains are illustrated. Red boxes identify markers used in this study.

SUPPLEMENTARY TABLES

Supplementary Table 1 - Serum-free differentiation medium (SFD) (100 ml)

	Ingredient	Volume	Source
1	DMEM	50 ml	Gibco 11960
2	F12	50 ml	Gibco 11765
	Supplement Mix [1]	**Concentration**	
3	Insulin	5 µg / ml	Sigma I9278
4	Transferrin	50 µg / ml	Sigma T1147
5	Na selenite	30 nM	Sigma S5261
6	putrescine	100 µM	Sigma P7505
7	progesterone	20 nM	Sigma P8783
8	hydrocortisone	20 nM	Sigma H0888
9	tri-iodothyronine	30 nM	Sigma T6397
10	Bovine Albumin	10 µg / ml	Sigma A6003

[1] The Supplement Mix was prepared as a 100x stock in DMEM. Ingredients 1-7 are components of N2 medium [Bottenstein and Sato, 1979]. Hydrocortisone and tri-iodothyronine support the survival and differentiation of astrocytes [Bottenstein, 1981; 1985; Morrison and deVellis, 1981; 1983] and oligodendrocytes [Barres et al., 1994; Jones et al., 2003], respectively.

Supplementary Table 2 - Antibodies used for cell phenotype analysis

Primary Antibodies	Dilution	Species	Source
Fixation with 4% paraformaldehyde			
anti-Brn3a	1:5000	rabbit	E. Turner[1]
anti-Engrailed-1 (4G11)	1:50	mouse	DSHB[2]
anti-Evx1 (99.1-3A2)	1:100	mouse	DSHB
anti-Hoxb4 (I12)	1:100	rat	DSHB
anti-Islet1 (39.4D5)	1:100	mouse	DSHB
anti-Lim1/2 (4F2)	1:100	mouse	DSHB
anti-nestin (RC2)	1:20	mouse	DSHB
anti-Nkx2.2 (74.5A5)	1:100	mouse	DSHB
anti-Nkx6.1 (F55A10)	1:100	mouse	DSHB
anti-Oct3/4 (SC 9081)	1:200	rabbit	Santa Cruz
anti-Pax2 (71-6000)	1:300	rabbit	Zymed
anti-Pax6 (PAX6)	1:200	mouse	DSHB
anti-Tbr1 (AB 9616)	1:3000	rabbit	Chemicon
anti-Tbr2 (AB 9618)	1:2000	rabbit	Chemicon
anti-β-3-tubulin (PRB-435P) (MMS-435P)	1:2000 1:2000	rabbit mouse	Covance
anti-vimentin (40E-C)	1:50	mouse	DSHB
anti-nestin (SCRR-1001)	1:1000	rabbit	ATCC
Fixation with 4% paraformaldehyde, 0.1% glutaraldehyde			
anti-GABA (A2052)	1:2000	rabbit	Sigma
anti-GAD (GAD-6)	1:50	mouse	DSHB
anti-GAP43 (AB 5220)	1:1200	rabbit	Chemicon
anti-GFAP (G6171)	1:1000	mouse	Sigma
anti-MAP2 (MAB 3418)	1:300	mouse	BM
anti-vGLUT1 (AB 5905)	1:5000	guinea pig	Millipore
Secondary Antibodies	**Dilution**	**Species**	**Source**
Cy2 or Cy3 anti-mouse IgG	1:400	goat	Chemicon
Cy2 or Cy3 anti-rabbit IgG	1:400	goat	Chemicon
Cy3 anti-rat IgG	1:400	goat	Chemicon
Alexa546 anti-mouse IgG1 or IgG2a	1:500	goat	Invitrogen
Alexa568 anti-guinea pig IgG	1:400	goat	Invitrogen
Alexa647 anti-mouse IgG1 or IgG2b	1:200	goat	Invitrogen
FITC anti-mouse IgM	1:100	goat	Sigma

[1] Fedtsova and Turner, 1995
[2] Developmental Studies Hybridoma Bank.

Supplementary Table 3 - Gene Function Enrichment Analysis: genes enriched in cell differentiated with SFD medium alone.

Genes ↑ in SFD	Genes on Chip	P-value	GO Term Name
9	53	0.000296	anterior/posterior pattern formation
11	83	0.000533	brain development
33	451	0.000566	cell differentiation
16	114	0.000016	chromatin binding
16	132	0.000090	chromatin modification
115	1810	<0.000001	DNA binding
11	60	0.000033	forebrain development
5	18	0.000795	histone-lysine N-methyltransferase activity
22	243	0.000319	mRNA processing
51	791	0.000409	multicellular organismal development
16	147	0.000297	negative regulation of transcription from RNA polymerase II promoter
21	203	0.000074	nervous system development
9	52	0.000258	neuron differentiation
79	1343	0.000206	nucleic acid binding
235	4025	<0.000001	nucleus
20	222	0.000622	positive regulation of transcription from RNA polymerase II promoter
132	1910	<0.000001	regulation of transcription, DNA-dependent
106	1414	<0.000001	transcription
15	138	0.000460	transcription activator activity
10	72	0.000662	transcription coactivator activity
57	847	0.000062	transcription factor activity
30	369	0.000184	transcription factor complex
22	225	0.000112	transcription regulator activity
7	32	0.000315	vasculogenesis
13	112	0.000596	Wnt receptor signaling pathway
108	2056	0.000913	zinc ion binding

Highlighted GO terms are plotted in Fig. 4A.

Supplementary Table 4 - Gene Function Enrichment Analysis: genes enriched in both RA-treated and untreated cells

Genes ↑ in SFD	Genes on Chip	P-value	GO Term Name
12	27	0.000367	ATP biosynthetic process
33	63	<0.000001	axon
25	71	0.000019	axon guidance
23	60	0.000011	cell soma
11	24	0.000493	cholesterol biosynthetic process
13	33	0.000651	coated pit
539	3226	<0.000001	cytoplasm
38	157	0.000477	cytoplasmic vesicle
82	424	0.000748	cytoskeleton
139	718	0.000013	endoplasmic reticulum
80	385	0.000106	endoplasmic reticulum membrane
12	28	0.000503	ER to Golgi vesicle-mediated transport
137	577	<0.000001	Golgi apparatus
64	262	0.000005	Golgi membrane
13	27	0.000099	growth cone
80	354	0.000007	GTP binding
38	161	0.000751	GTPase activity
29	104	0.000245	homophilic cell adhesion
55	229	0.000038	intracellular protein transport
26	92	0.000410	lipid biosynthetic process
794	5038	<0.000001	membrane
56	207	0.000001	microtubule
22	72	0.000402	microtubule associated complex
18	51	0.000253	microtubule binding
26	75	0.000017	microtubule-based process
66	301	0.000097	mitochondrial inner membrane
24	42	<0.000001	NADH dehydrogenase (ubiquinone) activity
24	39	<0.000001	NADH dehydrogenase activity
23	79	0.000578	negative regulation of cell cycle
51	203	0.000023	nervous system development
23	65	0.000037	neuron migration
21	58	0.000057	post-translational protein modification
781	4889	<0.000001	protein binding
101	479	0.000008	protein transport
21	61	0.000114	regulation of protein metabolic process
21	58	0.000057	small conjugating protein ligase activity
59	229	0.000003	small GTPase mediated signal transduction
11	24	0.000493	sterol biosynthetic process
48	208	0.000275	synapse
29	104	0.000245	transcription factor binding
98	442	0.000001	ubiquitin cycle
33	124	0.000221	ubiquitin-protein ligase activity
54	165	<0.000001	vesicle-mediated transport

Supplementary Table 5 - Gene Function Enrichment Analysis: genes enriched in cells differentiated with exposure to RA.

Genes ↑ in SFD	Genes on Chip	P-value	GO Term Name
10	27	0.000076	ATP biosynthetic process
12	35	0.000032	ATP synthesis coupled proton transport
21	105	0.000142	calcium ion transport
43	311	0.000408	cell junction
8	25	0.000996	cytochrome-c oxidase activity
11	36	0.000181	cytoskeletal protein binding
28	155	0.000070	endosome
108	577	<0.000001	Golgi apparatus
46	262	0.000001	Golgi membrane
16	50	0.000004	hydrogen ion transmembrane transporter activity
14	41	0.000008	hydrogen ion transporting ATP synthase activity, rotational mechanism
14	41	0.000008	hydrogen ion transporting ATPase activity, rotational mechanism
8	25	0.000996	hydrogen-exporting ATPase activity, phosphorylative mechanism
390	4074	0.000009	integral to membrane
33	229	0.000940	intracellular protein transport
61	500	0.000729	ion transport
25	138	0.000159	manganese ion binding
511	5038	<0.000001	membrane
5	8	0.000494	metalloendopeptidase inhibitor activity
107	909	0.000036	mitochondrion
9	20	0.000040	neurotransmitter secretion
17	69	0.000054	pattern specification process
5	7	0.000270	peptidyl-threonine phosphorylation
22	109	0.000088	postsynaptic membrane
7	17	0.000481	presynaptic membrane
68	479	0.000004	protein transport
19	59	<0.000001	proton transport
8	11	0.000004	proton-transporting ATP synthase complex, coupling factor F(o)
13	45	0.000085	proton-transporting two-sector ATPase complex
33	229	0.000940	small GTPase mediated signal transduction
45	208	<0.000001	synapse
6	10	0.000170	synaptic vesicle
14	55	0.000170	synaptosome
178	1641	0.000011	transport
10	26	0.000056	tricarboxylic acid cycle
33	165	0.000002	vesicle-mediated transport

Figure 4B Dendrogram Numerical Index:

1	RA		
2	RA vs SFD		
3	hippocampus	Affymetrix MOE430v2 GEO: GSM92512, GSM92513 and GSM92514 vs NSCs GSM272847 and GSM272848	
4	RA vs ES		
5	SFD vs ES		
6	cerebellum	Affymetrix MOE430v2 GEO: GSM205978 and GSM205979 vs NSCs GSM272847 and GSM272848	
7	zymogenic cells (aka chief cells)	Affymetrix MOE430v2 GEO: GSE5018(GSM113347)	[Ramsey et al., 2007]
8	lateral ventricle brain (LVBr) http://www.ebi.ac.uk/arrayexpress/	Affymetrix mgU74	[Ramalho-Santos et al., 2002] Accession: E-MEXP-1158
9	zymogenic cells (aka chief cells)	Affymetrix mu11K	[Mills et al., 2003]
10	retina http://giscompute.gis.a-star.edu.sg/suppdata_stemness/	Affymetrix mgU74	[Fortunel et al., 2003]
11	small intestine available upon request of L.V. Hooper	Affymetrix mu11K	[Hooper et al., 2001]
12	surface mucous cells (SMC) (aka stomach pit cells)	Affymetrix MOE430v2 GEO: GSM113348	[Ramsey et al., 2007]
13	skin	Affymetrix mgU74 GEO: GSM7478, GSM7479, GSM7480 Raw chip data available upon request of R.J. Feezor	[Feezor et al., 2004]
14	hematopoietic stem cells (HSC) http://www.ebi.ac.uk/arrayexpress/	Affymetrix mgU74	[Ramalho-Santos et al., 2002] Accession: E-MEXP-1158
15	hematopoietic stem cell ESTs (HSC-EST)		[Ivanova et al., 2002] Unigene Library 11946

16	hematopoetic stem cells (HSC)	Affymetrix mgU74	[Ivanova et al., 2002]
	http://www.cbil.upenn.edu/RAD3/php/displayStudy.php?study_id=270		
17	neural stem cells (NSC)	Affymetrix mgU74	[D'Amour & Gage, 2003]
	available upon request of F.H. Gage		
18	neural stem cells (NSC)	Affymetrix mgU74	[Ramalho-Santos et al., 2002]
	http://www.ebi.ac.uk/arrayexpress/		Accession: E-MEXP-1158
19	neural stem cells (NSC)	Affymetrix mgU74	[Ivanova et al., 2002]
	http://www.cbil.upenn.edu/RAD3/php/displayStudy.php?study_id=270		
20	mesenchymal stem cells ESTs (MSC-ESTs)		[Sharov et al., 2003]
			Unigene Library 10031
21	epidermal stem cells (epidermal SC)	Affymetrix mgU74	[Tumbar et al., 2004]
	http://www.rockefeller.edu/labheads/fuchs/database.php		
22	small intestine epithelial precursor (IEP)	Affymetrix mu11K	[Stappenbeck et al., 2003]
	http://gutsc.wustl.edu/supplement		
23	gastric epithelial progenitor (GEP)	Affymetrix mu11K	[Mills et al., 2002]
	http://gutsc.wustl.edu/supplement		
24	SFD		
25	colonic epithelial precursors (CEP)	MOE430	[Doherty et al., 2008]
		GEO: Pending	
26	SFD vs RA		
27	hepatic progenitor cells (HPC)	Affymetrix MOE430v2	[Ochsner et al., 2007]
		GEO: GSE6966	
28	neuroblast	Affymetrix mgU74	[Fortunel et al., 2003]
	http://giscompute.gis.a-star.edu.sg/suppdata_stemness/		

Figure S4 Dendrogram Numerical Index:

1	RA		
2	hippocampus	Affymetrix MOE430v2 GEO: GSM92512, GSM92513 and GSM92514 vs NSCs GSM272847 and GSM272848	
3	retina	Affymetrix mgU74	[Fortunel et al., 2003] http://giscompute.gis.a-star.edu.sg/suppdata_stemness/
4	lateral ventricles brain (LVBr)	Affymetrix mgU74 http://www.ebi.ac.uk/arrayexpress/	[Ramalho-Santos et al., 2002] Accession: E-MEXP-1158
5	cerebellum	Affymetrix MOE430v2 GEO: GSM205978 and GSM205979 vs NSCs GSM272847 and GSM272848	
6	SFD		
7	neuroblast	Affymetrix mgU74	[Fortunel et al., 2003] http://giscompute.gis.a-star.edu.sg/suppdata_stemness/
8	neural stem cells (NSC)	Affymetrix mgU74 available upon request of F.H. Gage	[D'Amour & Gage, 2003]
9	neural crest	Affymetrix mgU74 (non-differentiating media 48 hr) GEO: GSE1588 (GSM27271-4) vs LVBr	[Williams et al., 2007]
10	neural stem cells (NSC)	Affymetrix mgU74 http://www.cbil.upenn.edu/RAD3/php/displayStudy.php?study_id=270	[Ivanova et al., 2002]
11	neural stem cells (NSC)	Affymetrix mgU74 GEO: GSE587 (GSM8900 and GSM8904) vs LVBr	
12	neural stem cells (NSC)	Affymetrix mgU74 http://www.ebi.ac.uk/arrayexpress/	[Ramalho-Santos et al., 2002] Accession: E-MEXP-1158
13	embryonic stem cells (ESC)	Affymetrix mgU74 http://www.ebi.ac.uk/arrayexpress/	[Ramalho-Santos et al., 2002] Accession: E-MEXP-1158
14	ESC		

REFERENCES FOR SUPPLEMENTARY MATERIALS

Barres, B.A., Koroshetz, W.J., Swartz, K.J., Chun, L.L., Corey, D.P. 1990. Ion channel expression by white matter glia: the O-2A glial progenitor cell. Neuron. 4, 507-524.

Barres, B.A., Lazar, M.A., Raff, M.C. 1994. A novel role for thyroid hormone, glucocorticoids and retinoic acid in timing oligodendrocyte development. Devel. 120, 1097-1108.

Bottenstein, J.E. 1981. Proliferation of glioma cells in serum-free defined medium. Cancer Treat Rep. 65(Suppl 2), 67-70.

Bottenstein, J.E. Growth and Differentiation of Neural Cells in Defined Media. In: Bottenstein, J.E., Sato, G., (Eds.) Cell Culture in the Neurosciences, Plenum Press, New York, 1985, pp. 3-43.

Bottenstein, J.E., Sato, G.H. 1979. Growth of a rat neuroblastoma cell line in serum-free supplemented medium. Proc. Natl. Acad. Sci. USA. 76, 514-517.

Conti L, Pollard SM, Gorba T, Reitano E, Toselli M, Biella G, Sun Y, Sanzone S, Ying QL, Cattaneo E, Smith A. 2005. Niche-independent symmetrical self-renewal of a mammalian tissue stem cell. PLoS Biol. 3, e283.

D'Amour, K.A., Gage, F.H. 2003. Genetic and functional differences between multipotent neural and pluripotent embryonic stem cells. Proc. Natl. Acad. Sci. USA. 100 (Suppl 1), 11866-11872.

Doherty, J.M., Geske, M.J., Stappenbeck, T.S., Mills, J.C. 2008. Diverse adult stem cells share specific higher-order patterns of gene expression. Stem Cells. 26, 2124-2130.

Fedtsova, N.G., Turner, E.E. 1995. Brn-3.0 expression identifies early post-mitotic CNS neurons and sensory neural precursors. Mech. Dev. 53, 291-304.

Feezor, R.J., Paddock, H.N., Baker, H.V., Varela, J.C., Barreda, J., Moldawer, L.L., Schultz, G.S., Mozingo, D.W. 2004. Temporal patterns of gene expression in murine cutaneous burn wound healing. Physiol. Genom. 16, 341-348.

Fortunel, N.O., Otu, H.H., Ng, H.H., Chen, J., Mu, X., Chevassut, T., Li, X., Joseph, M., Bailey, C., Hatzfeld, J.A., Hatzfeld, A., Usta, F., Vega, V.B., Long, P.M., Libermann, T.A., Lim, B. 2003. Comment on " 'Stemness': transcriptional profiling of embryonic and adult stem cells" and "a stem cell molecular signature". Science. 302, 393.

Hooper, L.V., Wong, M.H., Thelin, A., Hansson, L., Falk, P.G., Gordon, J.I. 2001. Molecular analysis of commensal host-microbial relationships in the intestine. Science. 291, 881-884.

Ivanova, N.B., Dimos, J.T., Schaniel, C., Hackney, J.A., Moore, K.A., and Lemischka, I.R. 2002. A stem cell molecular signature. Science. 298, 601-604.

Jones, S.A., Jolson, D.M., Cuta, K.K., Mariash, C.N., Anderson, G.W. 2003. Triiodothyronine is a survival factor for developing oligodendrocytes. Mol. Cell. Endocrinol. 199, 49-60.

Li, M., Pevny, L., Lovell-Badge, R., Smith, A. 1998. Generation of purified neural precursors from embryonic stem cells by lineage selection. Curr. Biol. 8, 971-974.

Mills, J.C., Andersson, N., Hong, C.V., Stappenbeck, T.S., Gordon, J.I. 2002. Molecular characterization of mouse gastric epithelial progenitor cells. Proc. Natl. Acad. Sci. USA. 99, 14819-14824.

Mills, J.C., Andersson, N., Stappenbeck, T.S., Chen, C.C., Gordon, J.I. 2003. Molecular characterization of mouse gastric zymogenic cells. J. Biol. Chem. 278, 46138-46145.

Morrison, R.S., de Vellis, J. 1981. Growth of purified astrocytes in a chemically defined medium. Proc. Natl. Acad. Sci. USA. 78, 7205-7209.

Morrison, R.S., de Vellis, J. 1983. Differentiation of purified astrocytes in a chemically defined medium. Brain Res. 285, 337-345.

Ochsner, S.A., Strick-Marchand, H., Qiu, Q., Venable, S., Dean, A., Wilde, M., Weiss, M.C., Darlington, G.J. 2007. Transcriptional profiling of bipotential embryonic liver cells to identify liver progenitor cell surface markers. Stem Cells. 25, 2476-2487.

Ramalho-Santos, M., Yoon, S., Matsuzaki, Y., Mulligan, R.C., Melton, D.A. 2002. "Stemness": transcriptional profiling of embryonic and adult stem cells. Science. 298, 597-600.

Ramsey, V.G., Doherty, J.M., Chen, C.C., Stappenbeck, T.S., Konieczny, S.F., Mills, J.C. 2007. The maturation of mucus-secreting gastric epithelial progenitors into digestive-enzyme secreting zymogenic cells requires Mist1. Devel. 134, 211-22.

Sharov, A.A., Piao, Y., Matoba, R., Dudekula, D.B., Qian, Y., VanBuren, V., Falco, G., Martin, P.R., Stagg, C.A., Bassey, U.C., Wang, Y., Carter, M.G., Hamatani, T., Aiba, K., Akutsu, H., Sharova, L., Tanaka, T.S., Kimber, W.L., Yoshikawa, T., Jaradat, S.A., Pantano, S., Nagaraja, R., Boheler, K.R., Taub, D., Hodes, R.J., Longo, D.L., Schlessinger, D., Keller, J., Klotz, E., Kelsoe, G., Umezawa, A., Vescovi, A.L., Rossant, J., Kunath, T., Hogan, B.L., Curci, A., D'Urso, M., Kelso, J., Hide, W., Ko, M.S. 2003. Transcriptome analysis of mouse stem cells and early embryos. PLoS Biol. 1, E74.

Stappenbeck, T.S., Mills, J.C., Gordon, J.I. 2003. Molecular features of adult mouse small intestinal epithelial Progenitors. Proc. Natl. Acad. Sci. USA. 100, 1004-1009.

Tumbar, T., Guasch, G., Greco, V., Blanpain, C., Lowry, W.E., Rendl, M., Fuchs, E. 2004. Defining the epithelial stem cell niche in skin. Science. 303, 359-363.

Williams, S.S., Mear, J.P., Liang, H.C., Potter, S.S., Aronow, B.J., Colbert, M.C. 2004. Large-scale reprogramming of cranial neural crest gene expression by retinoic acid exposure. Physiol. Genom. 19, 184-197.